NAVAL POSTGRADUATE SCHOOL

MONTEREY, CALIFORNIA

THESIS

EFFECT OF SPAN VARIATION ON THE PERFORMANCE OF A CROSS FLOW FAN

by

Charla W. Schreiber

June 2006

Thesis Advisor: Garth V. Hobson
Second Reader: Knox T. Millsaps

Approved for public release; distribution is unlimited

THIS PAGE INTENTIONALLY LEFT BLANK

REPORT DOCUMENTATION PAGE			Form Approved OMB No. 0704-0188
Public reporting burden for this collection of information is estimated to average 1 hour per response, including the time for reviewing instruction, searching existing data sources, gathering and maintaining the data needed, and completing and reviewing the collection of information. Send comments regarding this burden estimate or any other aspect of this collection of information, including suggestions for reducing this burden, to Washington headquarters Services, Directorate for Information Operations and Reports, 1215 Jefferson Davis Highway, Suite 1204, Arlington, VA 22202-4302, and to the Office of Management and Budget, Paperwork Reduction Project (0704-0188) Washington DC 20503.			
1. AGENCY USE ONLY ***(Leave blank)***	**2. REPORT DATE** June 2006	**3. REPORT TYPE AND DATES COVERED** Master's Thesis	
4. TITLE AND SUBTITLE Effect of Span Variation on the Performance of a Cross Flow Fan		**5. FUNDING NUMBERS**	
6. AUTHOR(S) Schreiber, Charla W.			
7. PERFORMING ORGANIZATION NAME(S) AND ADDRESS(ES) Naval Postgraduate School Monterey, CA 93943-5000		**8. PERFORMING ORGANIZATION REPORT NUMBER**	
9. SPONSORING /MONITORING AGENCY NAME(S) AND ADDRESS(ES) N/A		**10. SPONSORING/MONITORING AGENCY REPORT NUMBER**	
11. SUPPLEMENTARY NOTES The views expressed in this thesis are those of the author and do not reflect the official policy or position of the Department of Defense or the U.S. Government.			
12a. DISTRIBUTION / AVAILABILITY STATEMENT Approved for public release; distribution is unlimited		**12b. DISTRIBUTION CODE**	

13. ABSTRACT (maximum 200 words)

Over the past few decades, advances in aeronautic and control technologies have established a new vision for future air transportation systems. NASA has initiated the motion with several programs supporting the "highway of the sky," a system of launch pads and air pathways enabling smaller and more easily piloted aircraft to travel the open space above instead of busy freeways and crowded city streets.

Previous investigations into crossflow fan technology as a propulsion source have identified its potential for use in personal aircraft and vertical takeoff and landing applications. To further development, performance characteristics must be determined for the possible configurations and under variable conditions to understand factors critical to design.

This experiment studied flow characteristics of a crossflow fan incorporating 30 blades of six inch length in a six inch diameter rotor. Comparison was made against the performance of a fan of similar design but one-fourth the length span previously tested. Results were plotted for various parameters along constant speed lines of operation and general trends were determined. These results were used to quantitatively deduce scaling relationships for this device.

14. SUBJECT TERMS Crossflow fan, cross flow fan, personal air vehicle propulsion			**15. NUMBER OF PAGES** 65
			16. PRICE CODE
17. SECURITY CLASSIFICATION OF REPORT Unclassified	**18. SECURITY CLASSIFICATION OF THIS PAGE** Unclassified	**19. SECURITY CLASSIFICATION OF ABSTRACT** Unclassified	**20. LIMITATION OF ABSTRACT** UL

NSN 7540-01-280-5500 Standard Form 298 (Rev. 2-89)
Prescribed by ANSI Std. 239-18

THIS PAGE INTENTIONALLY LEFT BLANK

Approved for public release; distribution is unlimited

EFFECT OF SPAN VARIATION ON THE PERFORMANCE OF A CROSS FLOW FAN

Charla W. Schreiber
Lieutenant, United States Navy
B.S., United States Naval Academy, 1999

Submitted in partial fulfillment of the
requirements for the degree of

MASTER OF SCIENCE IN MECHANICAL ENGINEERING

from the

NAVAL POSTGRADUATE SCHOOL
June 2006

Author: Charla W. Schreiber

Approved by: Garth V. Hobson
Thesis Advisor

Knox. T. Millsaps
Second Reader/Co-Advisor

Anthony J. Healey
Chairman, Department of Mechanical and Astronautical Engineering

THIS PAGE INTENTIONALLY LEFT BLANK

ABSTRACT

Over the past few decades, advances in aeronautic and control technologies have established a new vision for future air transportation systems. NASA has initiated the motion with several programs supporting the "highway of the sky," a system of launch pads and air pathways enabling smaller and more easily piloted aircraft to travel the open space above instead of busy freeways and crowded city streets.

Previous investigations into crossflow fan technology as a propulsion source have identified its potential for use in personal aircraft and vertical takeoff and landing applications. To further development, performance characteristics must be determined for the possible configurations and under variable conditions to understand factors critical to design.

This experiment studied flow characteristics of a crossflow fan incorporating 30 blades of six inch length in a six inch diameter rotor. Comparison was made against the performance of a fan of similar design but one-fourth the length span previously tested. Results were plotted for various parameters along constant speed lines of operation and general trends were determined. These results were used to quantitatively deduce scaling relationships for this device.

THIS PAGE INTENTIONALLY LEFT BLANK

TABLE OF CONTENTS

THIS PAGE INTENTIONALLY LEFT BLANK

LIST OF FIGURES

THIS PAGE INTENTIONALLY LEFT BLANK

LIST OF TABLES

THIS PAGE INTENTIONALLY LEFT BLANK

ACKNOWLEDGMENTS

With sincerest gratitude I would like to acknowledge the following:

For his patience, guidance, and inspiration, without which this work would not be possible, Dr. Garth Hobson. From the classroom where he instructed with contagious enthusiasm, to the laboratory where he skillfully engineered and trialed project by project, Dr. Hobson is the balance of professional researcher and passionate educator. His ethic has left many lasting impressions and hopes to emulate.

For his exacting standards and constant reliability, Dr. Knox Millsaps. As I have learned, the toughest critics are often the ones who care the most.

For their technical expertise and boundless help, John Gibson and Rick Still. They can make anything work, and make anything fun.

For being my family away from home, Ke Kai O`Uhane.

And lastly, for their understanding and constant love, Ku`u`ino, Mana, and Sagesse.

THIS PAGE INTENTIONALLY LEFT BLANK

I. INTRODUCTION

A. OVERVIEW

As civilian aeronautic technology advances at an astounding rate, air travel has conquered many obstacles once thought impossible. With such recent achievements as the Airbus 380 (an 850-passenger capable airliner with a 560 mph cruising speed) and the sub-orbital space flight of the civilian craft SpaceShipOne in 2004, aircraft technology has hit its zenith. Therefore it is somewhat ironic that another trend in the aeronautic sector has been toward development of much smaller and lower flying aircraft that would seem unimpressive compared to these recent breakthroughs. This is, however, a logical and necessary direction for growth, because it aims to solve certain existing needs that cannot be met by these record breaking aircraft.

In recent years the groundwork has begun for a "highway in the sky," where the next generation of the automobile will also be able to taxi onto a runway and takeoff into the skies above, leaving traffic and stoplights behind. Led by NASA's efforts to develop and test the ground control systems, airframes, avionics, and propulsion advancements needed for its inception, this system may be the next great advancement in air travel. This movement has been envisioned as a solution to America's escalating traffic congestion problems in many cities as well the growing transportation demand from business commuters [Ref. 1]. There could also be global demand for this type of system, as world populations steadily increase and place similar stresses on current transportation infrastructures.

With an emphasis on vehicles with shorter takeoff and landing distances and piloting systems that are nearly automated or as simplified as driving an automobile, more efficient use could be made of the airspace and runways this system will serve providing for a large volume of air commuters. Furthermore, vertical takeoff and landing (VTOL) would be the safest launch arrangement for these aircraft, eliminating the potentially dangerous mix of high airspeed and proximity to other aircraft and terrain that currently requires skilled piloting and ground control. Coupled with more affordable

composite materials and engine technology becoming available every day, personal air vehicles could allow the average person to be commuting to work in the air in the near future.

As for the technology behind a personal air vehicle of the future, many concepts have been demonstrated to be feasible and prototypes have already been built that hold promise for consumer production. Moller International has successfully built and flown a "Volantor" deemed the Skycar, for instance, a vehicle using four, directed-thrust, ducted fans to produce both lift and propulsion [Ref. 2]. Though this design has demonstrated reasonably good capability and efficiency, there remains other undeveloped mechanisms for lift generation and propulsion with potentially better characteristics.

The crossflow fan (CFF) is one propulsion device with a strong potential for VTOL applications, because of the structural and dimensional flexibility and efficiency it has shown. Several concepts have thus far been proposed for utilizing crossflow fans in aircraft. In one design, the Fanwing [Ref. 3], which incorporates a crossflow fan into the leading edge of a wing section, flight tests have already demonstrated successful application in short takeoff and landing (STOL). Still, more refined testing in addition to what has already been conducted would be necessary before a prototype VTOL aircraft could be built around this device. The experiment carried out in this study expanded on previous tests by operating a crossflow fan rotor of similar configuration but extended length to confirm airflow characteristics and determine applicable lengthwise scaling rules.

B. BACKGROUND

The basic crossflow fan design has been in existence for over a century, utilized in applications from computer cooling fans to the ventilation of refrigerated compartments of modern grocery stores. In both cases, the desired fluid inflow or outflow is a wide but thin field, which suggested the use of such a device. Thus, one attraction to this type of fan is its dimensional characteristics, a relatively small diameter rotor with extendable length for increased output. In the case of aircraft propulsion, other aspects of the crossflow fan become valued. Because of its simple rotary operation and easily scaled diameter, it can be powered by more readily available engines and be

incorporated almost anywhere in the aircraft where a drive shaft can be fitted. Furthermore, flow direction can easily be controlled by thrust vectoring since the fan seems to have no specific angular requirements for inlet and exit positions. Also, when fully encased, the operation of a crossflow fan would be far less hazardous than current unshrouded propellers or helicopter rotors.

The first serious look at crossflow fans for aircraft lift occurred in 1975 at the Vought Systems Division (VSD) of LTV Aerospace Corporation when a Navy contract was awarded for their study [Ref. 4]. During these tests, a total of 46 configurations of various rotor arrangements and external housing geometries were evaluated for fans of 12-inch diameter, and either 1.5- or 12-inch span. For the rotor, different blade angles and number of blades were tested, and changes were made to the pressure cavities and exit ducting within the housing. The position and shape of these pressure cavities were varied to help control the effects of a vortex which develops in the flow, and thus impacted the efficiency of the fan during operation. Results of the testing determined that one particular configuration of the Multi-Bypass Ratio Propulsion System, namely the #8 assembly, operated with the best power efficiency. The schematic of this fan within its cavities and inlet and exhaust sections is shown in Figure 1.

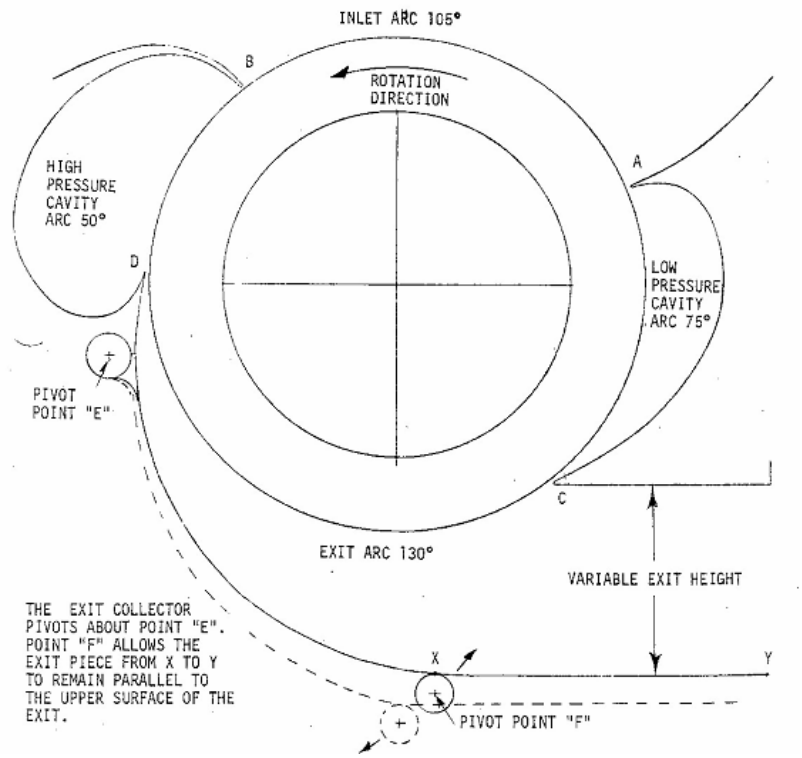

Figure 1. VSD multi-bypass ratio propulsion system #8 assembly (From Ref. 1)

Because of a wane in interest towards VTOL capability by the Navy after the 1980s, the program was not further pursued. With a spark of inspiration driven by NASA's "highway in the sky" programs, and emergence of concept designs for personal air vehicles, however, interest in CFF technology was reinvigorated earlier in this decade. Researchers at the Naval Postgraduate School's Turbopropulsion Laboratory (TPL) opened a new chapter on crossflow fans in 2000, when Gossett [Ref. 5], proposed a concept design for a single seat, lightweight, VTOL aircraft including two, directed-thrust, ducted fans augmented with a crossflow fan for lift. He derived the thrust requirements for this fan as well as weight and power constraints from the VSD data. Later, a series of tests were conducted on a 12-inch diameter, 1.5-inch length fan similar to the VSD assembly #8 by Seaton and Cheng in 2003 [Refs. 6 and 7]. This rotor is shown in Figure 2. Initial testing validated the results of the VSD tests and incorporated other testing methods to provide further insight into the fan's performance. Specifically, beyond baseline tests, pressure cavities were blanked and throttling was added to the exhaust ducting to vary mass flow rate. Additionally, flow visualization was performed

with dye-marker injection through the blanking plate to monitor patterns of flow in the rotor. In [Ref. 8], further calculations were made from this data to determine the length of fan needed to provide lift to Gossett's concept aircraft. Finally, a 6-inch diameter, 1.5-inch span rotor was tested and compared against its 12-inch counterpart [Ref. 9]. In these latter tests, efficiencies above 70% were achieved for various throttle conditions (thus for certain mass flow rates) when speeds were between 3000-6000 RPM. Below these speeds, significantly lower efficiencies were apparent, though higher thrust-to-power values were obtained.

Figure 2. Twelve inch by one and one half inch crossflow fan tested at NPS TPL (From Ref. 3)

Retaining the same base configuration as these previous experiments, the current rotor was extended in length to a 6-inch span in order to determine lengthwise scaling relationships pertinent to this device. Also, in consideration of operating at greatest efficiency levels during real-world application, these tests focused on a speed range between 3000-6000 RPM. The experimental data obtained were then compared to the previous 6-inch diameter, 1.5-inch span rotor tested and effects of lengthwise scaling determined.

THIS PAGE INTENTIONALLY LEFT BLANK

II. EXPERIMENT

A. CROSSFLOW FAN CONFIGURATION AND TESTING APPARATUS

1. Crossflow Fan Test Assembly (CFTA)

The configuration of the crossflow fan studied here was derived from previous fans tested at NPS TPL, including similar blade forms and angles, number of blades, and construction. Specifically, the fan rotor consisted of a one-inch thick machined disc as the base which mounted onto the drive shaft with countersunk screws. The 30 blades were initially weighed and ordered into a pattern which minimized effects on rotational balance. They were positioned between the base and outer end plate and fixed in place using metal dowels into preset holes and further bonded with high strength epoxy. A modification of the unsupported end was made to the previous rotor design in attempt to provide lengthwise stability during high rotation speeds in view of the increased rotor span from 1.5 inches to 6 inches. In this rotor, a solid disc, as shown in Figure 3, was substituted for the retaining ring at the free end. At the center of this disc was a spindle that seated into the blanking plate of the housing assembly through a sealed bearing. This change aimed to mechanically support the previously free end and thus dampen oscillation of the rotor about its longitudinal axis.

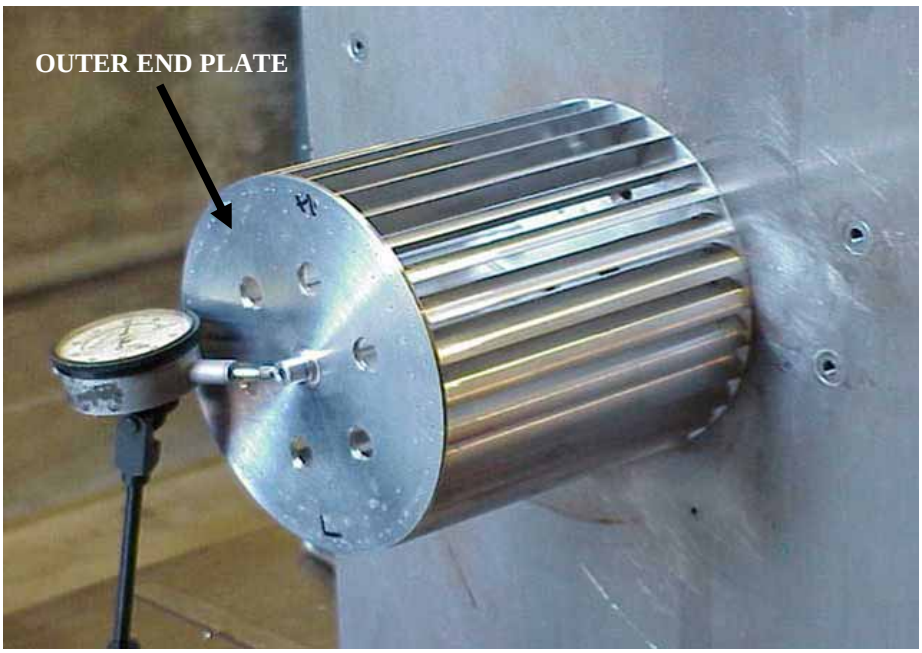

Figure 3. Assembled crossflow fan rotor installed on the drive shaft

The housing assembly was constructed with two end walls (front and back) that were bolted onto the test bench. To the backwall plate was mounted a set of machined forms which created the high and low pressure cavities, and the remaining side plates needed to form a closed chamber. With the rotor mounted onto the drive shaft, the front wall was installed and bolted in place. Into this front wall a removable end plate (blanking plate) was fitted which contained pressure taps that could be rotated to change positions within the flow. Also, in previous CFTAs, this blanking plate could be replaced with a Plexiglas window for observing flow visualizations. Due to the modifications made to this rotor, however, flow visualizations were no longer possible. Also, labyrinth seals around the side edge of the rotor base as well as the end plate of the front housing wall helped minimize flow losses in these gaps. Figure 4 displays the assembly with front wall mounted but blanking plate removed.

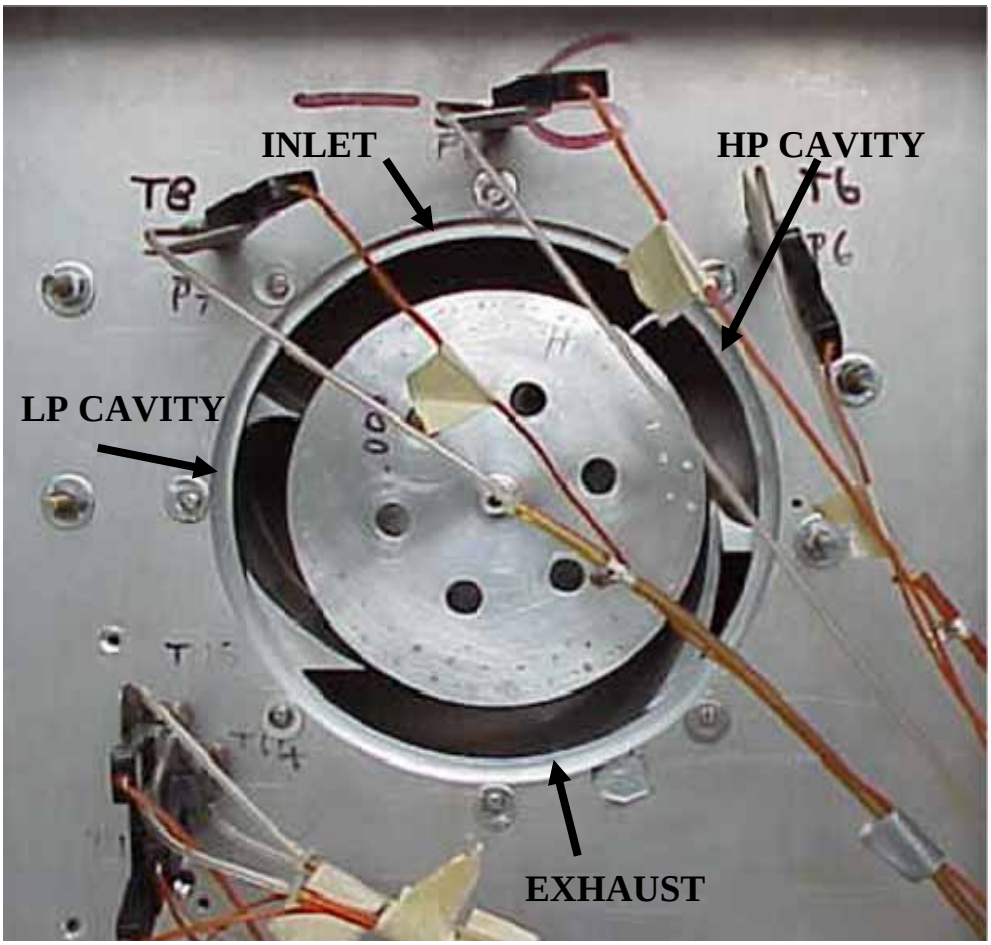

Figure 4. Partially assembled crossflow fan assembly

Next a plenum chamber was situated atop the housing structure, from which the inlet could be fitted with additional pipe ducting leading up to a bellmouth nozzle. With the inlet elliptical bellmouth mounted, mass flow measurements could be determined from the averaged pressure reading at its throat as shown in Figure 5. Lastly, exhaust ducting was mounted to the exit section to incorporate a butterfly valve for throttling studies. These additions allowed for measuring and reducing mass flow rate through the control volume, allowing a compressor map to be made through the range of operating speeds. A side view of the housing assembly and exit duct is shown in Figure 6, where the flow centerline positioning of the probe tips is visible.

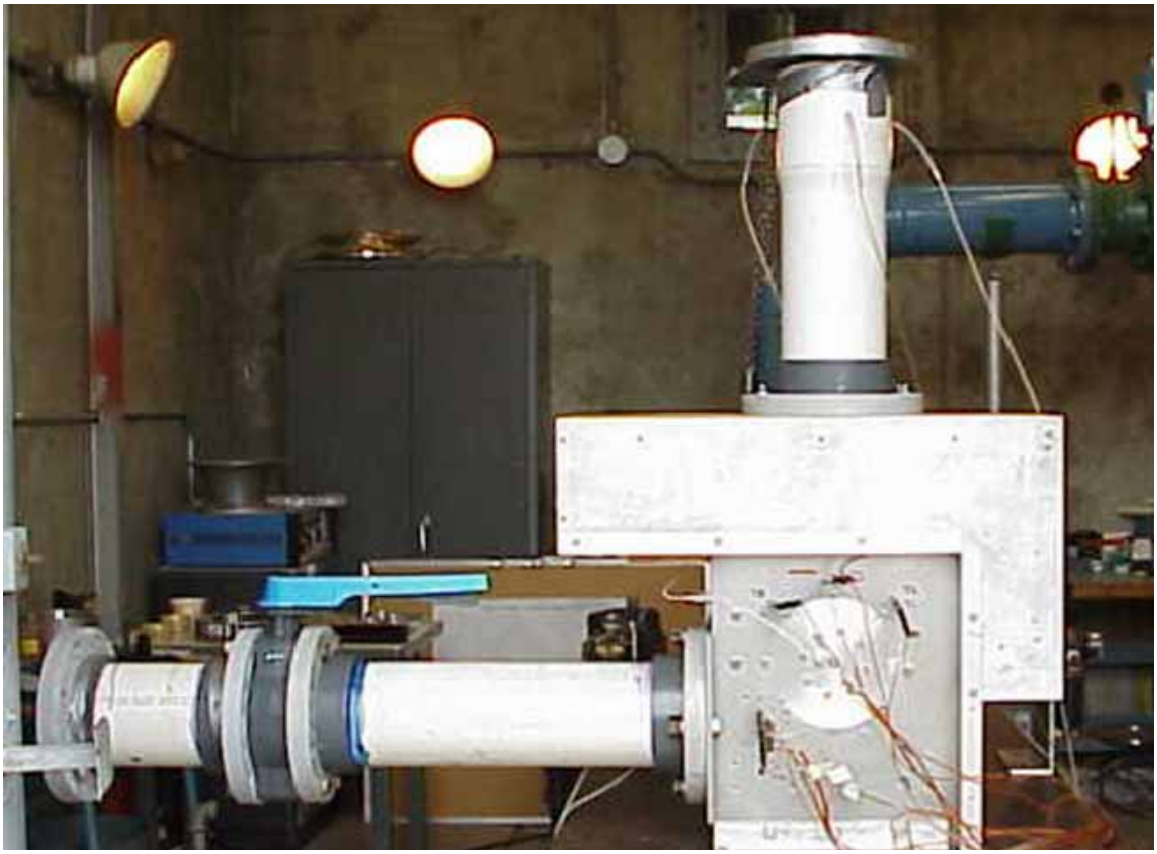

Figure 5. Crossflow fan test assembly

Figure 6. Side view of crossflow fan test assembly

2. Turbine Test Rig

Providing power to the drive shaft of the CFTA was a turbine which was driven by the air supply system of an Allis-Chalmers 12-stage axial compressor driven by a 1,250-horsepower engine. Producing 10,000 cubic feet per minute of air at 30 psig, the system routed compressed air through piping into the test cell's plenum chamber. An air/water heat exchanger in line also cooled the supply to slightly above ambient temperature. Additionally, a pressurized oil mister system provided lubrication for both the turbine portion and the CFTA drive shaft bearing.

A data acquisition system provided bearing temperatures, vibration monitoring and speed (by a once-per-revolution monitor) through the turbine.

B. CONTROLS AND INSTRUMENTATION

1. Control Procedure

From the control station overlooking the test cell (Figure 7), flow from the plenum chamber was throttled by butterfly valves to the turbine or out through a discharge line (dumping to the atmosphere) to achieve desired rotational speed of the drive turbine. This speed was monitored through the once-per-revolution signal from the drive turbine. As the flow was increased between test runs to the next higher speed, usually in 500 or 1000 RPM increments, minor valve adjustments were made and the flow allowed to be steadied before data was collected for that run. A window next to the control station also provided for visual monitoring of the test cell during the run.

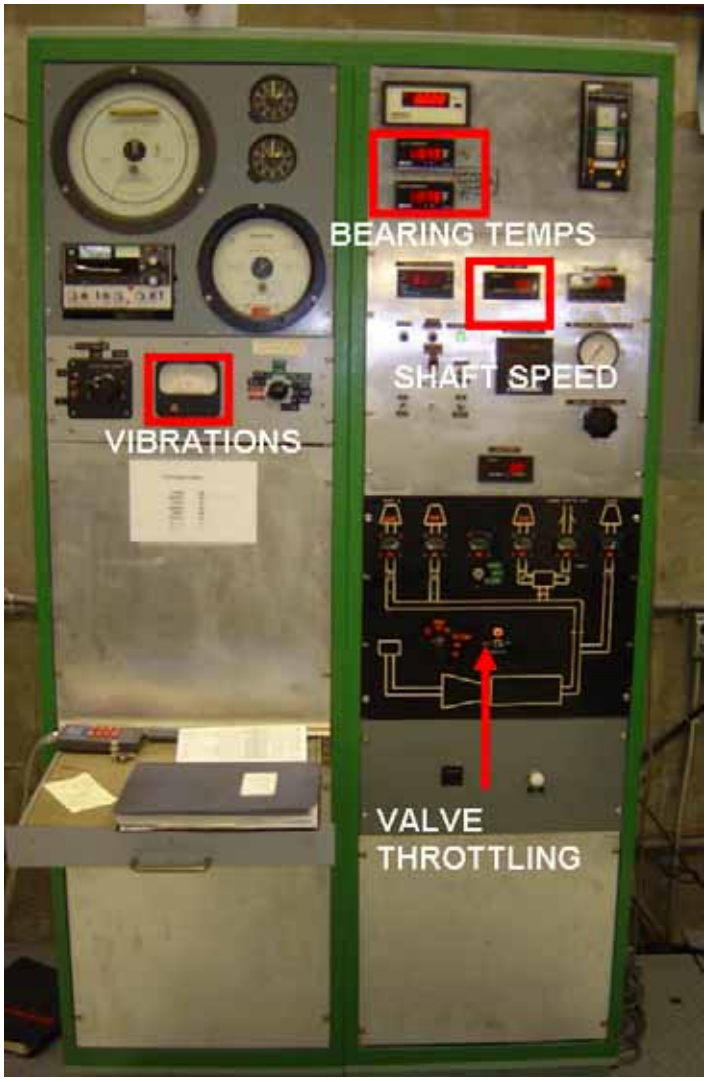

Figure 7. Control station

The data required to determine performance of the CFF was obtained by pressure and temperature probes positioned throughout the control volume around the crossflow fan test assembly. These consisted of static pressure taps, thermocouple probes, or combination total pressure/thermocouple probes. Static pressure taps were located around the inlet bellmouth and in various locations along the inner walls of the housing chamber, while combination probes were situated along the centerline of the flow field in the inlet section (at the 10, 12, and 2 o'clock positions from fan center) and along the exit section (top, middle, and bottom positions). Locations of these probes are shown in Figure 8. Thermocouple probes were also situated along the length of the drive turbine to monitor temperatures during operation. Pressure measurements were taken inside the test cell and in the control room (to determine an atmospheric reference). Furthermore, several vibration sensors were mounted on the front wall of the CFTA housing as well as the drive turbine to monitor vibrations and frequency effects during trial runs of the CFF.

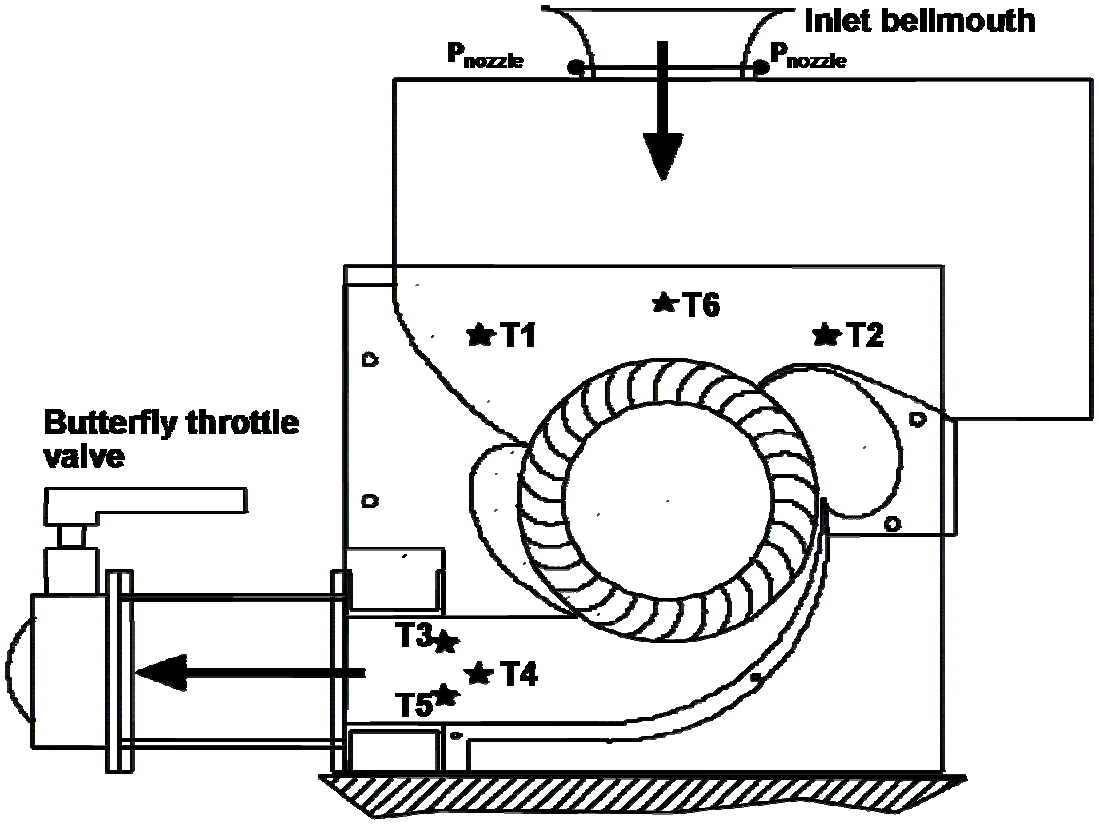

Figure 8. Probe and port locations (After Ref. 6)

C. DATA ACQUISITION SYSTEM

1. Hardware

The data acquisition system consisted of equipment in the control room which interfaced the sensor lines emerging from the CFTA with the PC-based HPVEE program. The system diagram is found in Figure 9. Within the test cell, air tubes from the pressure probes and static pressure taps led to a Scanivalve controller/ transducer, which converted mechanical pressures into electronic signals for routing back to the scanning multiplexer in the control room. Similarly, the thermocouple sensor wires were routed to the thermocouple multiplexer. Lastly, a counter-totalizer in the rack converted electric pulses from the once-per-revolution monitor on the drive turbine into a readout of shaft speed. The Scanivalve pressure ports and thermocouple multiplexer channel assignments are listed in Tables 1 and 2. Several port and channel assignments from previous test assemblies were not used in current data reduction calculations but remained in the test plan for monitoring purposes only.

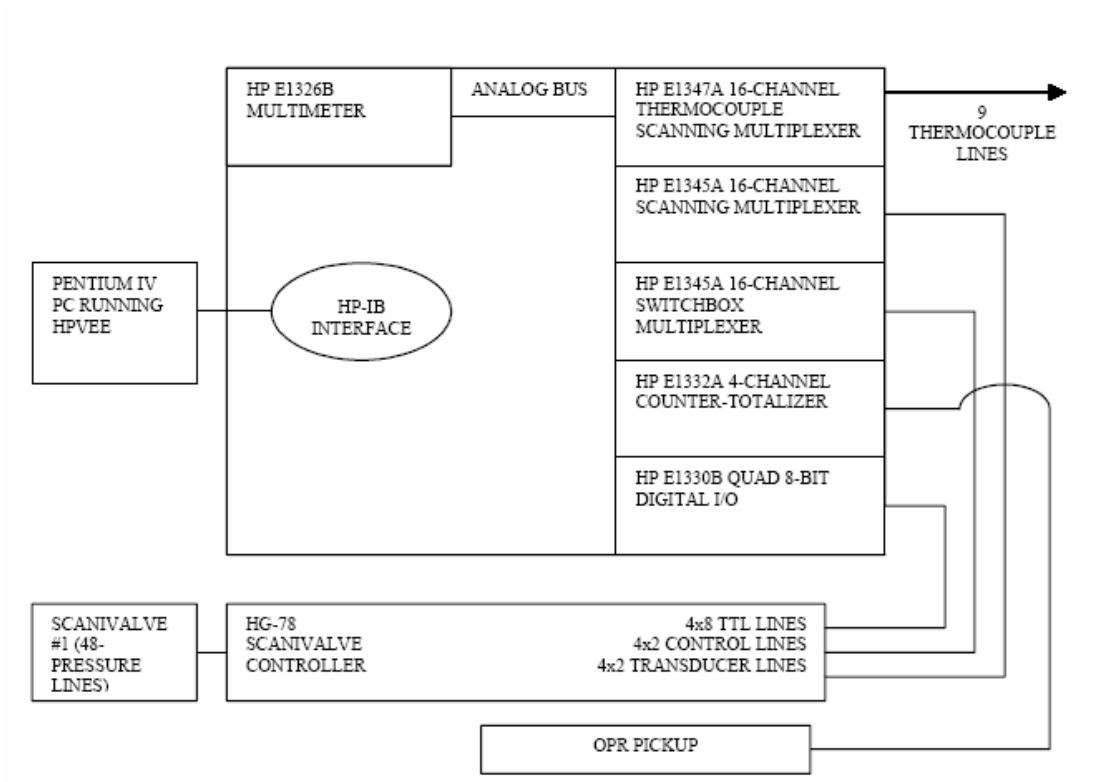

Figure 9. Data acquisition hardware diagram (From Ref. 3)

Port #	Sensor Type	Nomenclature
1	Static	P_{ATMOS}
2	Static	P_{CAL}
3	Total	P_{in}TTR (5 o'clock)
4	Total	P_{out}TTR
5	Total	P_{in}TTR (8 o'clock)
6	Total	P_{in}CFF (2 o'clock)
7	Total	P_{in}CFF(10 o'clock)
8	Total	P_{out}CFF(Top)
9	Total	P_{out}CFF(Mid)
10	Total	P_{out}CFF(Btm)
11	Static	P_{CELL}
12	Static	$P_{WALL\ OUTLET}$
13	Static	P_C
14	Static	P_D
15	Static	P_E
16	Static	P_{out}CFF
17	Static	P_G
18	Total	P_{in}CFF(12 o'clock)
19	Static	P_I
20	Static	P_J
21	Static	P_K
22	Static	P_L
24	Static	$P_{noz}1$
25	Static	$P_{noz}2$
26	Static	$P_{noz}3$
32	Static	P_{in}
33	Static	P_{in}(Flange)
34	Static	P_{out}(Flange)
35	Static	P_{out}(Vena)

Table 1. Scanivalve port assignments
(After Ref. 4)

Multiplexer Channel	Nomenclature
6	T_{in}CFF (2 o'clock)
7	T_{in}CFF(12 o'clock)
8	T_{in}CFF(10 o'clock)
9	T_{in}TTR (8 o'clock)
10	T_{in}TTR (5 o'clock)
11	T_{out}TTR
12	T_{in}Orifice
13	T_{out}CFF(Btm)
14	T_{out}CFF(Mid)
15	T_{out}CFF(Top)

Table 2. Thermocouple multiplexer channel assignments (After Ref. 4)

Before beginning a test run, the pressure signal was calibrated by assigning a specified voltage difference between channels of the reference pressure (port #2, set at a gage pressure of 5 inHg) and the ambient pressure measured in the control room (port #1). In this way, measurements made for each run were accurate for the specific conditions of that day.

2. Software

A program called CFF written in HPVEE, running on a Pentium-IV PC, was used to generate the control signals directing the Scanivalve to sequentially sample port pressures and to record data from the multiplexers and other devices. Once the complete set of raw data from all combination pressure and temperature probes and static pressure taps was received, HPVEE performed the necessary data reduction using formulated MATLAB scripts and output these values to a text file. These output files were then imported into Microsoft EXCEL for further data sorting and graphing tasks. A sample of the test-scheme architecture is found in Figure 10.

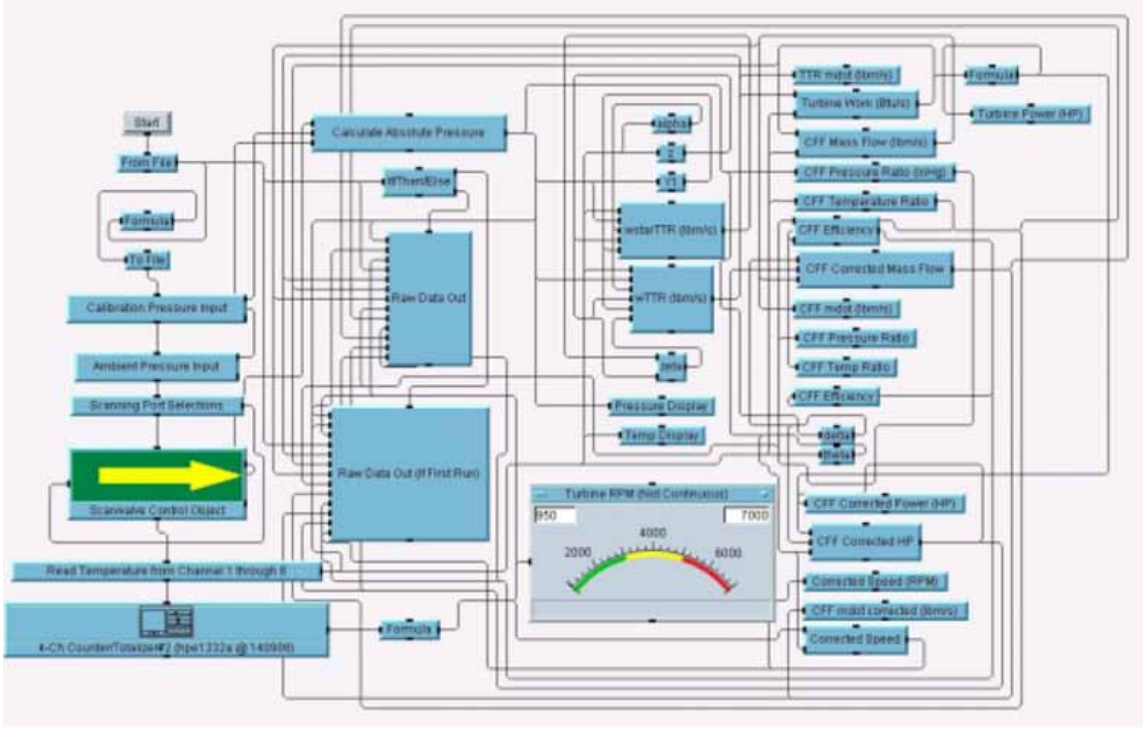

Figure 10. CFF HPVEE back-plane flow chart (From Ref. 3)

3. Data Reduction

The calculations of performance were based on equations found in [Ref. 10] and modified by [Ref. 6]. A summary of the more important relationships is given below.

The constants and properties of air used in these calculations were:

$$R = 287 \text{ J/kg-}^{o}\text{K} \qquad c_p = 1005 \text{ J/kg-}^{o}\text{K} \qquad \gamma = 1.41$$

$$P_{ref} = 101{,}325 \text{ Pa} \qquad T_{ref} = 15\ ^{o}\text{C}$$

In general, temperatures and pressures at sections of the cross flow fan were computed from an average of the measured values from the probes in that section. For example, at the inlet section of the CFF:

$$T_{in,CFF(avg)} = \frac{T_1 + T_2 + T_6}{3}$$

In the exit region, however, it was determined during previous tests that a profile developed along the height of the exit duct due to viscous wall effects. Thus, a mass averaging technique was used instead of a straight average. This included weighing each probe's measurements according to an area ratio of the cross section, where areas 1 and 3

represented the portion of flow sensed by the top and bottom probes, and area 2 by the middle probe. These ratios were determined to be:

$$A_1 = A_3 = 0.38889 A_{exit} \qquad A_2 = 0.2222 A_{exit}$$

Therefore the mass flow rate seen by each probe was calculated by the following:

$$\rho_i = \rho_{total} = \frac{P_i}{\left(RT_i\right)}\left(\frac{P_{outlet}}{P_i}\right)^{1/\gamma}$$

$$u_i = \sqrt{2c_p T_i}\left(\frac{P_{outlet}}{P_i}\right)^{(\gamma-1)/\gamma}$$

$$\dot{m}_i = \rho_i u_i A_i$$

Here P_i and T_i represented the total pressure and temperature for each of the three probes at the outlet of the CFF. Thus, the final averaged value of exit pressure and temperature were found by:

$$P_{out,CFF(m.avg)} = \frac{\dot{m}_1 P_{out,CFF(top)} + \dot{m}_2 P_{out,CFF(mid)} + \dot{m}_3 P_{out,CFF(btm)}}{\dot{m}_{tot}}$$

$$T_{out,CFF(m.avg)} = \frac{\dot{m}_1 T_{out,top} + \dot{m}_2 T_{out,mid} + \dot{m}_3 T_{out,btm}}{\dot{m}_{tot}}$$

The mass flow rate through the fan was determined using the density and velocity at the throat of the inlet bellmouth nozzle given its fixed cross section:

$$\dot{m}_{CFF} = \rho_{noz} u_{noz} A$$

With the density and velocity calculated respectively by:

$$\rho_{noz} = \frac{P_{noz}}{\left(RT_{noz}\right)} \qquad u_{noz} = \sqrt{\frac{\left(P_{cell} - P_{noz}\right)}{\frac{1}{2}\rho_{noz}}}$$

The total-to-total pressure and temperature ratios were found by:

$$\pi_{CFF} = \frac{P_{out,CFF(avg)}}{P_{in,CFF(avg)}} \quad \text{and} \quad \tau_{CFF} = \frac{T_{out,CFF(avg)}}{T_{in,CFF(avg)}}$$

Then, compression efficiency was calculated using the values obtained from above:

$$\eta_{CFF} = \frac{\pi_{CFF}^{\left(\frac{\gamma-1}{\gamma}\right)} - 1}{\tau_{CFF} - 1}$$

Correction of certain parameters for standard atmospheric conditions required the following equations:

$$N_{corr} = \frac{N}{\sqrt{\theta}}\ ,\quad \dot{m}_{corr} = \dot{m}\frac{\sqrt{\theta}}{\delta}\ ,\quad P_{corr} = \frac{P}{\delta\sqrt{\theta}}$$

$$\delta = \frac{P_{in,CFF(avg)}}{P_{ref}},\ \text{and}\ \ \theta = \frac{T_{in,CFF(avg)}}{T_{ref}}$$

Power into the CFF was calculated using the corrected mass flow rate, the constant pressure specific heat of air, and the temperature rise between inlet and outlet:

$$\dot{W}_{CFF} = \dot{m}_{CFF} c_P (T_{out,CFF(avg)} - T_{in,CFF(avg)})$$

Then, the exit velocity was determined:

$$u_{exit} = \sqrt{2c_p T_{out,CFFavg}} \left(\frac{P_{outlet}}{P_{out,CFFavg}} \right)^{(\gamma-1)/\gamma}$$

And finally, the corrected thrust was found:

$$F_{corr} = \dot{m}_{corr} * u_{exit}$$

D. TEST PLAN

Only a baseline configuration for the CFTA including exit valve throttling was used in this experiment (no cavity blanking) since the main effort of this study was a comparison against a shorter span rotor of the same diameter tested previously. The procedure of a trial run included sampling data at 1,000 and 2,000 RPM for initial checks of sensor readings, then proceeding with test runs between the desired range of 3,000 and 6,000 RPM, in either 500 or 1,000 RPM increments. Exhaust throttling was used to vary mass flow rates at a given speed to determine a total performance map for this CFF. This

was done by advancing the exit butterfly valve through notched positions until a stall condition was determined (drastic drop in efficiency). Finally, data reduction was conducted by HPVEE and used to plot selected parameters along operating lines for comparison. The parameters of interest to this study were the total-to-total pressure and temperature ratios, efficiency, corrected mass flow rate per unit span, corrected power, and corrected thrust.

THIS PAGE INTENTIONALLY LEFT BLANK

III. RESULTS

A. OVERVIEW

Raw and reduced data obtained during the test trials are found in the appendix, while graphical results are shown below. As discussed in the test plan section, trials were to be made for this crossflow fan between 3,000 and 6,000 RPM to compare its performance against previously conducted studies on a 6-inch diameter, 1.5-inch span rotor. However, during the fifth day of test run operation of the assembly, serious vibrations occurred as speed was increased above 4,700 RPM which caused catastrophic failure of the crossflow fan and resulted in irreparable damage to the rotor. Subsequent trials at speeds above 4,500 rpm were therefore not made because of time constraints. In view of this lack of desired data, comparison was then made for 2,000, 3,000, 4,000, and 4,500 RPM operating speeds against the shorter span crossflow fan.

Overall, these data which were obtained before destruction of the rotor indicated consistent trends with previous experiments and allowed for a glimpse of spanwise scaling effects.

B. PERFORMANCE OF 6-INCH SPAN ROTOR

1. Pressure and Temperature Ratios

Figures 11 and 12 highlight the operation of this rotor in view of total-to-total pressure and temperature ratios versus mass flow rate. The second order trendlines were of nearly uniform appearance and increased in magnitude as expected. Pressure ratios reached almost 1.035 when run at 4,500 RPM. In calculations made from the data collected by Seaton and Cheng [Refs. 6 and 7] and later by Gannon and Hobson [Ref. 9], a 12-inch diameter rotor running at 3,000 RPM produced a pressure ratio of about 1.04. This operating point was used to estimate the length of a crossflow fan needed to lift the early concept aircraft design developed by Gossett [Ref. 2], as well as the power required for operation. Therefore, should this smaller diameter rotor be incorporated into such a design, an operating point at 1.040 pressure ratio would require a speed somewhere about 5,000 RPM.

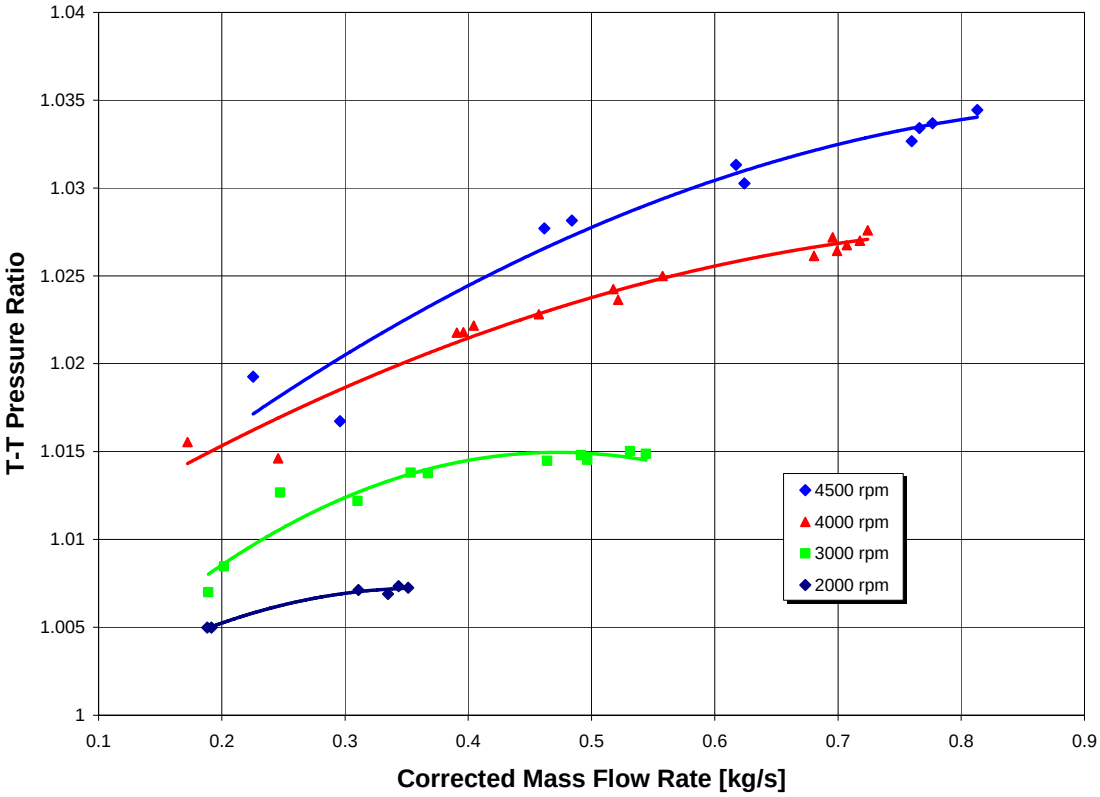

Figure 11. Total-to-total pressure ratio versus corrected mass flow rate

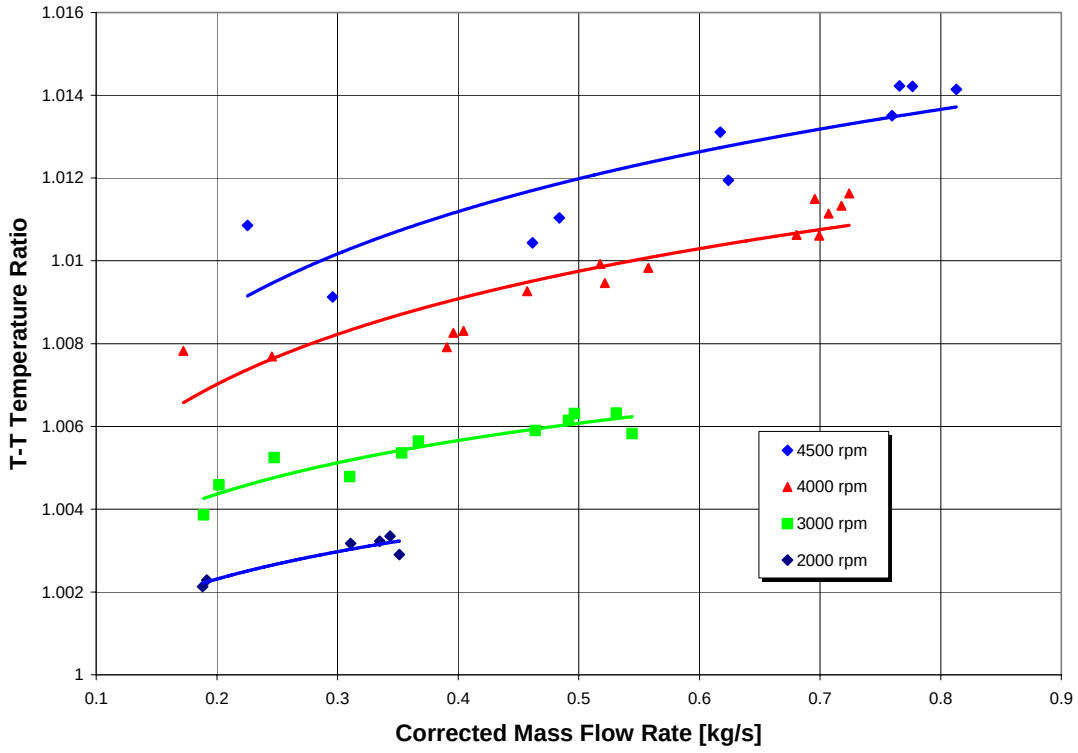

Figure 12. Total-to-total temperature ratio vs. corrected mass flow rate

2. Efficiency

Efficiency was charted in Figure 13 and demonstrated favorable values for the 6-inch span rotor. Peak percentages occurred in mid 70s range while speed was at 4,000 RPM, though data were inconsistent and scattered for the 2,000 RPM trials. This was expected because of the very low pressure and temperature ratios at this speed. Of note was the increase in efficiency as the exit valve was throttled from open to the 2-1/2 notch position, seen as the mass flow rate reduced along a speed line. Once this setting was passed, stall conditions were apparent in the rotor and efficiencies dropped drastically. This was also apparent in Figure 14, where efficiency was plotted against corrected speed for each exit valve setting. In this case, an average was made of all data points taken at a specific speed and throttle setting, then trendlines drawn for each throttle notch position to demonstrate effects of operating at reduced mass flow rates. Again, the 2-1/2 notch position maintained the overall efficiency, while open, 1-, and 2- notch setting lines showed moderate efficiencies and the 3rd notch setting showed very poor efficiencies indicating stall.

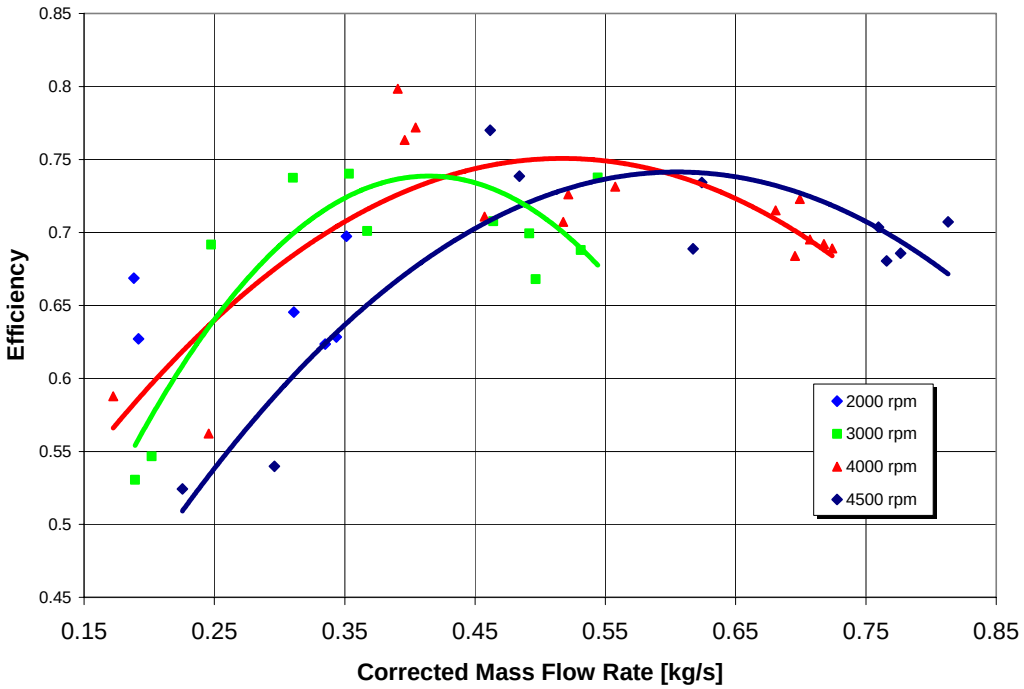

Figure 13. Efficiency versus corrected mass flow rate

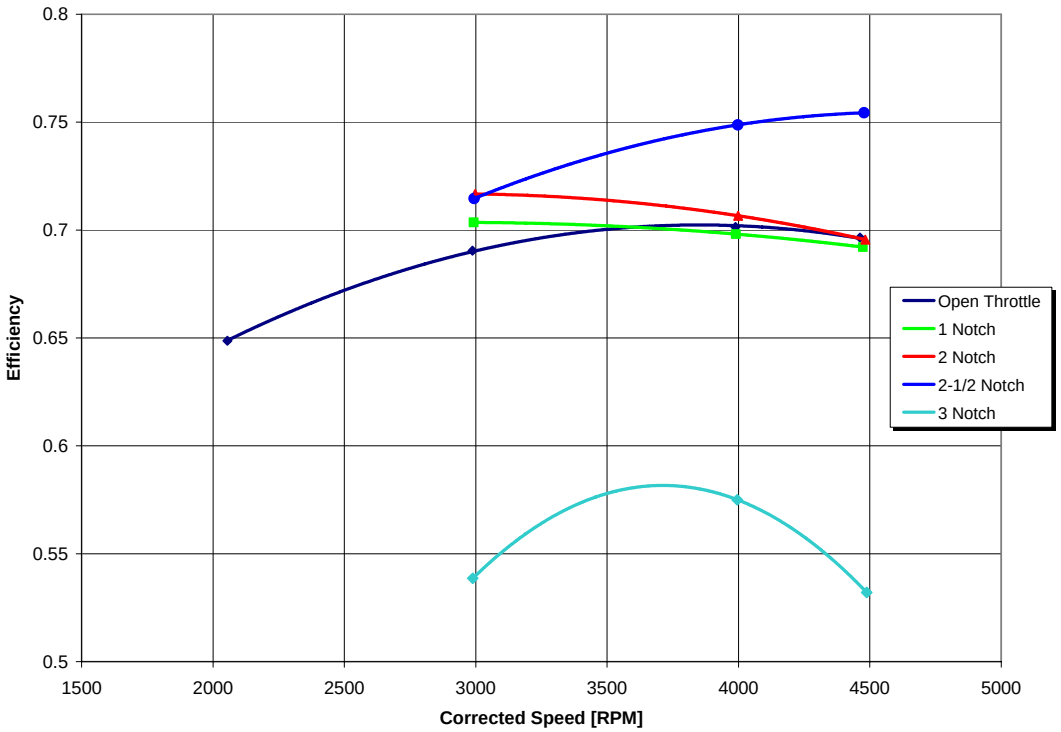

Figure 14. Efficiency versus corrected speed

3. Mass Flow Rate

Next, in Figure 15, corrected mass flow rate was plotted against corrected speed, again by exit valve notch position. Very straight, steady-growth trendlines with increased slope at the lower notch settings indicated that mass flow output of the fan was linear as expected.

4. Power

Corrected power was the next parameter investigated, as shown in Figure 16, where its unit length values were plotted against corrected speed by exit throttle notch setting. Power required by the CFF increased at a nearly exponential rate according to speed, a typical behavior for this parameter in a rotary device.

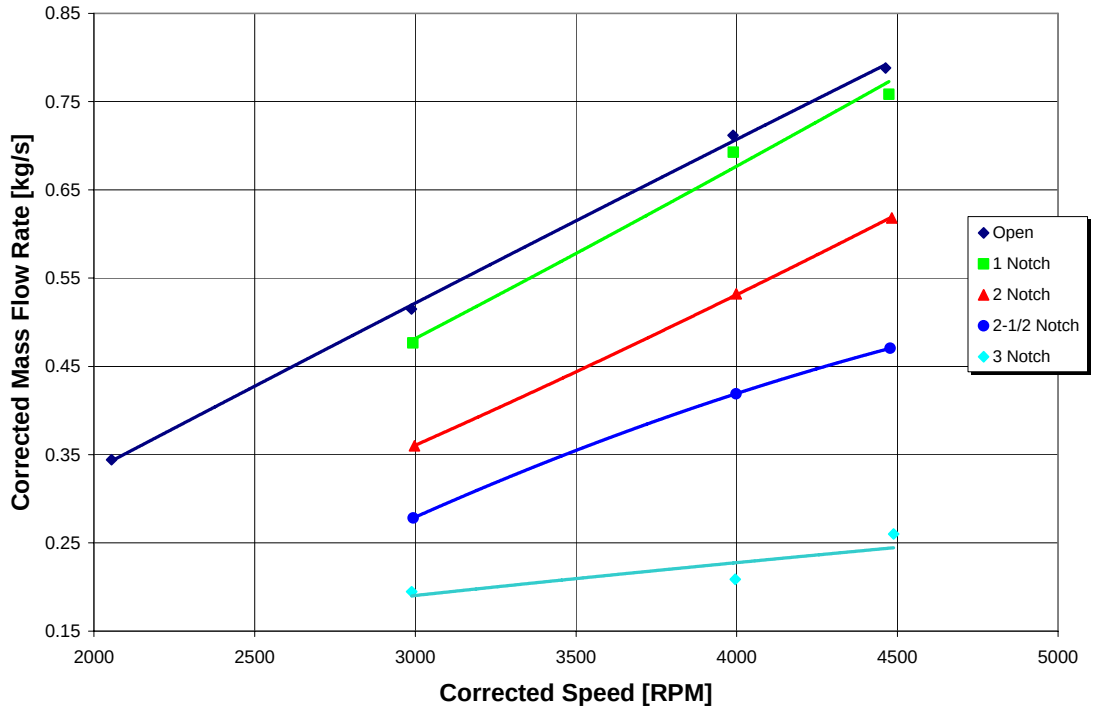

Figure 15. Corrected mass flow rate versus corrected speed

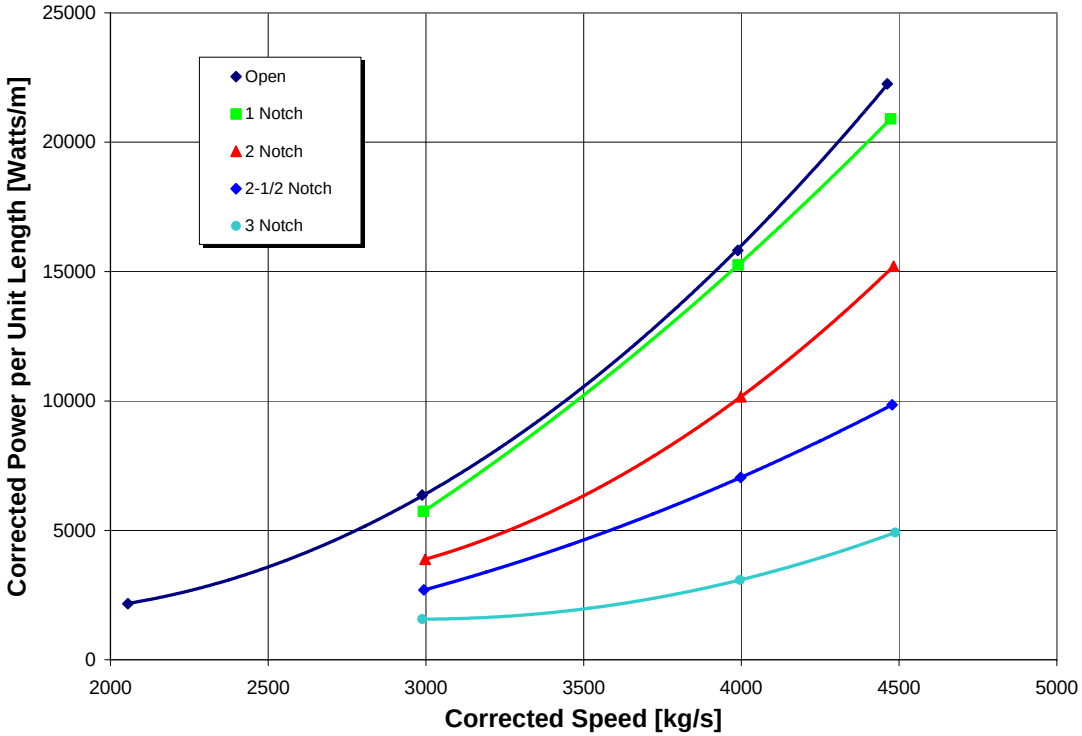

Figure 16. Corrected power versus corrected speed

5. Thrust

In Figures 17 and 18, thrust calculations were made for the 6-inch rotor versus corrected speed and corrected power, respectively. Indications were that operation at higher speeds showed greater thrust outputs, consistent with the effect of higher mass flows and exit velocities at those speeds. However, this came at the cost of decreasing thrust-to-power performance charted in the latter figure as power drawn increased with operating speed. This graph indicated a maximum thrust-to-power ratio in the vicinity of 150 N/m to 6,000 Watts, after which point a decreasing slope eroded this proportion.

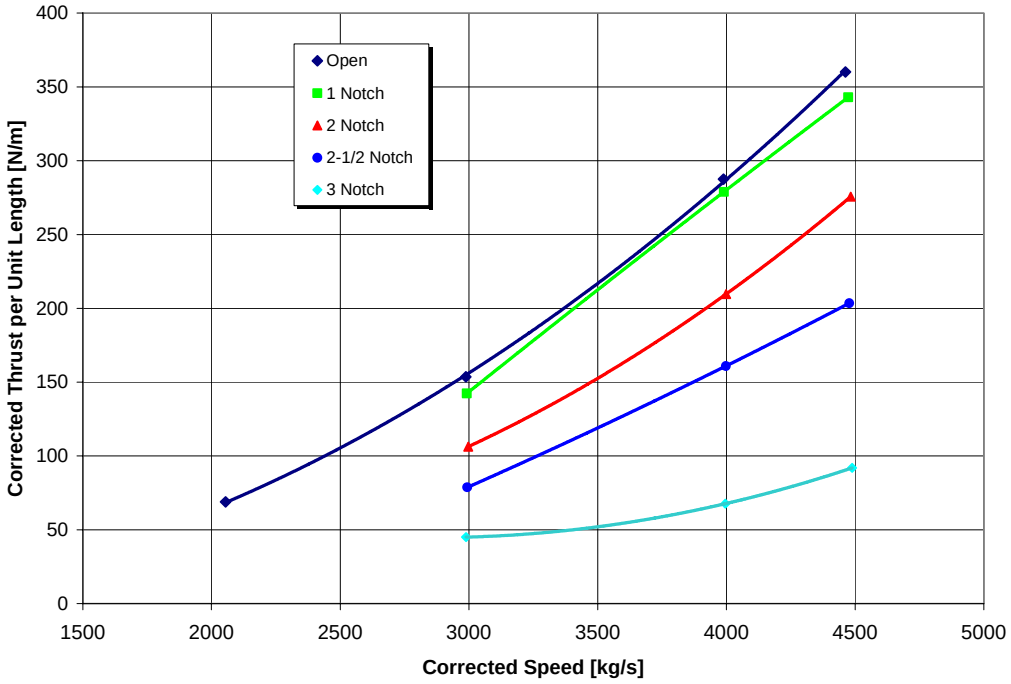

Figure 17. Corrected thrust versus corrected speed

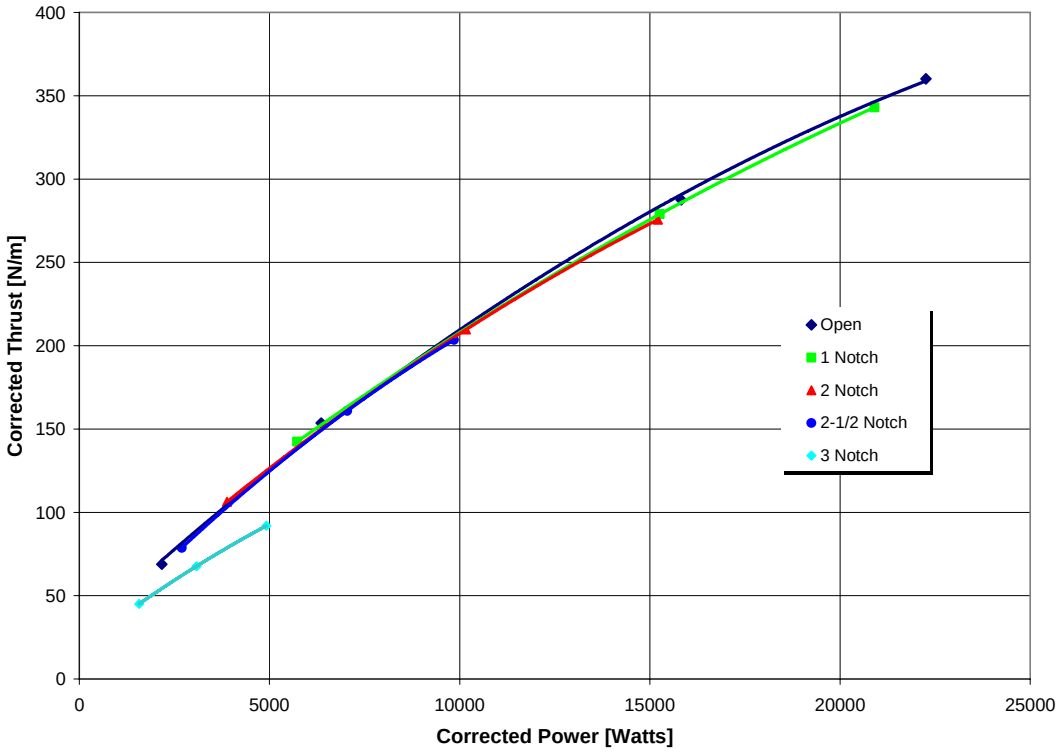

Figure 18. Corrected thrust versus corrected power

C. PERFORMANCE COMPARISON OF ROTORS

1. Pressure Ratios

Figure 19 shows the comparison of pressure ratios for both fans. At the 2,000 and 3,000 RPM speeds, data points of the shorter span fan are closely below the 6-inch rotor's performance line. Note that trendlines were drawn down by the stall points at the left ends of the curves. More realistically, though, the actual performance would remain high along an operating line until experiencing a sharp decline in pressure ratio when the stall occurred. At 4,000 RPM, the shorter span's data points seem to be slightly above the 6-inch fan operating line, but not significantly.

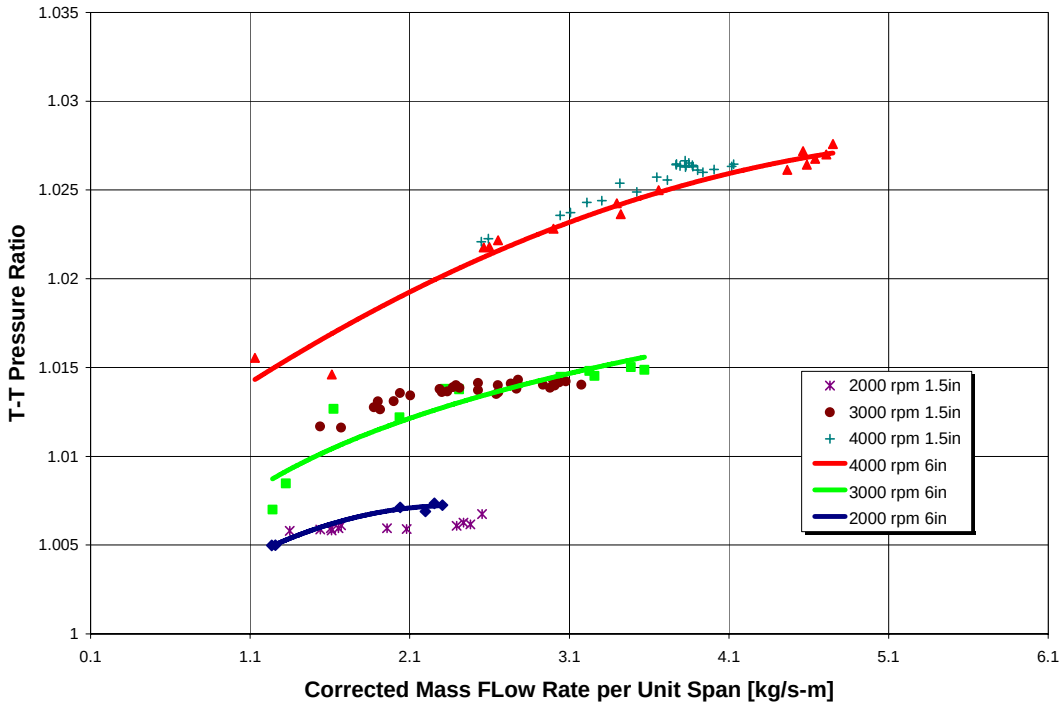

Figure 19. Comparison of pressure ratios versus corrected mass flow rate

2. Efficiency

In Figure 20 efficiencies were compared between the 6-inch and 1.5-inch spans and displayed with trendlines for the longer span and data points for the shorter span. As expected, the larger rotor maintained overall higher efficiencies at every speed, which was credited to its increased volume but similar wall surface area when compared to the shorter span rotor. Since frictional effects at the walls contributed to decreased efficiencies, poorer efficiencies were expected for the shorter fan, whose proportion of wall surface area to volume is greater than that for the 6-inch fan. For each, however, the 2,000 RPM data were not plotted as scatter and inconsistencies in both made it difficult to determine a trend.

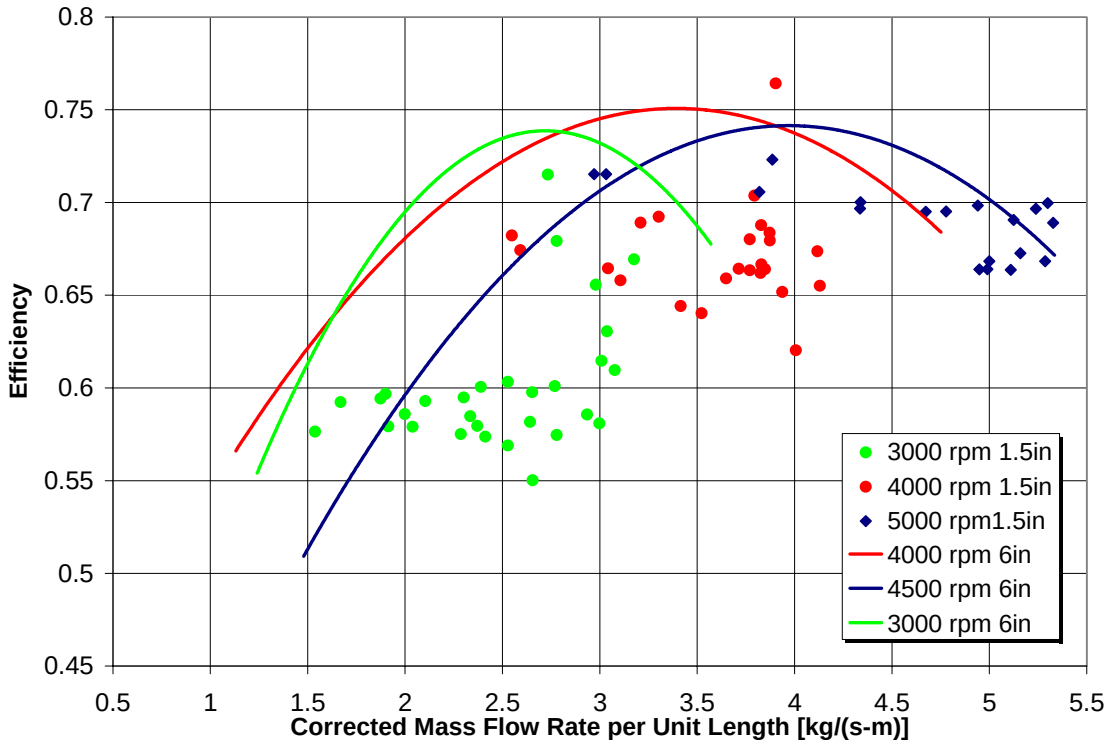

Figure 20. Comparison of fan efficiencies versus corrected mass flow rate

3. Mass Flow Rate per Unit Span

Comparison of mass flow rates per unit span was made in Figure 21. As anticipated, the 6-inch span rotor, whose upper trendline represented the open throttle, or maximum output setting, achieved higher rates of mass flow everywhere except at the 2000 RPM speed against the 1.5-inch span rotor. At this slow rate of operation, probe insensitivities to very slight changes in pressures and temperatures between the inlet and exit may have led to larger error margins in calculations. As the speed was increased, a distinct ratio of maximum output between the fans emerged as shown by the separation in trendlines. This ratio was determined to be approximately 0.86:1 above 3,000 RPM.

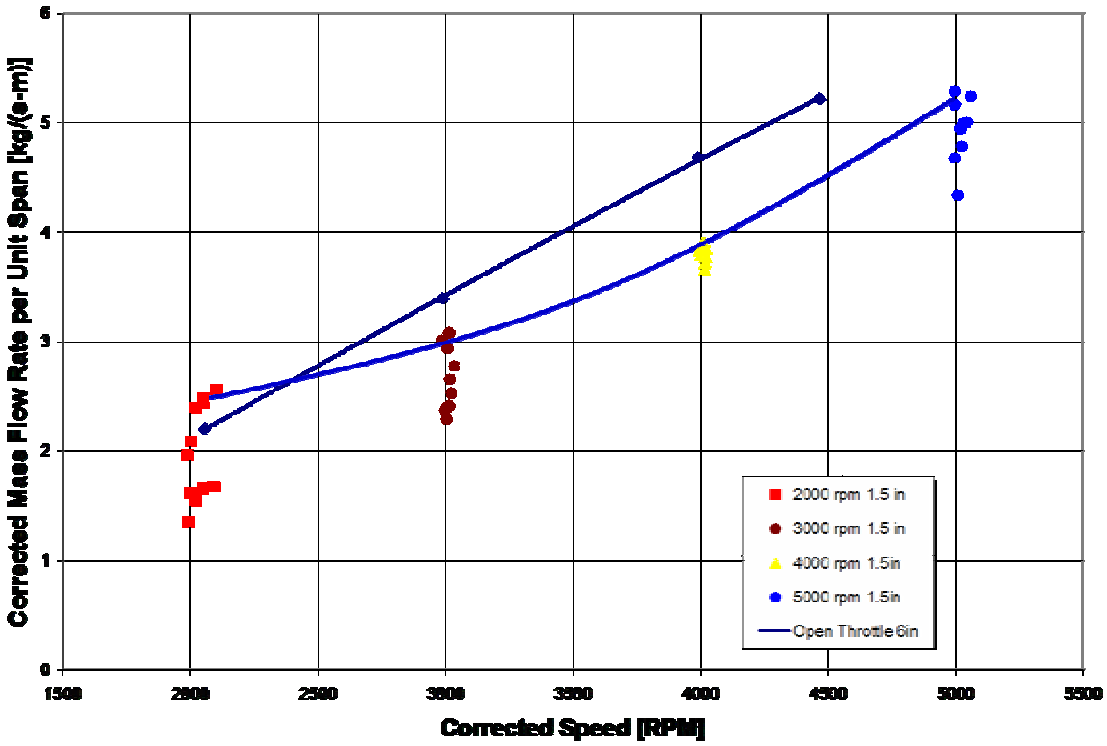

Figure 21. Comparison of mass flow rate per unit span versus corrected speed

4. Power

Corrected power versus corrected mass flow rate per unit length is shown in Figure 22 for the comparison. The graph indicated that the reduced span rotor consistently drew more power per mass flow per unit length above 2,000 RPM. Again, this was an expected outcome due to larger inefficiencies in its operation.

5. Thrust

Thrust per unit length versus corrected mass flow rate per unit length was compared in Figure 23, and indicated a very consistent performance between the 1.5-inch and 6-inch rotors as seen by the overlapping data points along each speed line. This resulted in a scaling factor of one for this parameter, and demonstrated that thrust per mass flow rate was unaffected by length scaling. This parameter would more so depend on variations of diameter due to its relationship with exit velocity, which would be increased with a larger diameter rotor.

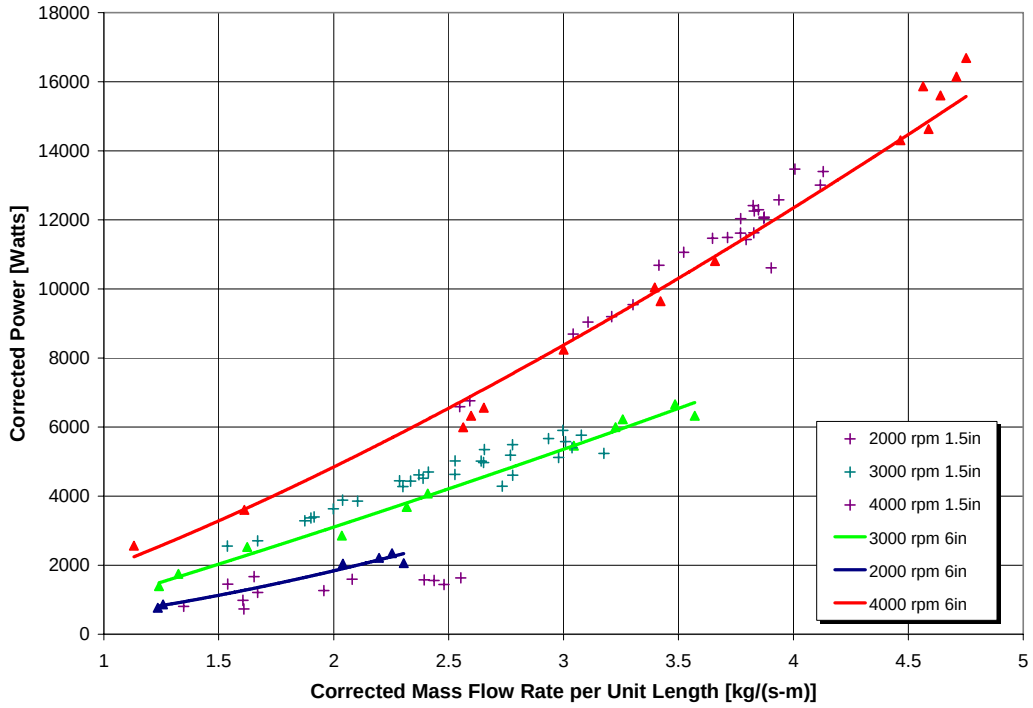

Figure 22. Comparison of corrected thrust versus corrected mass flow rate

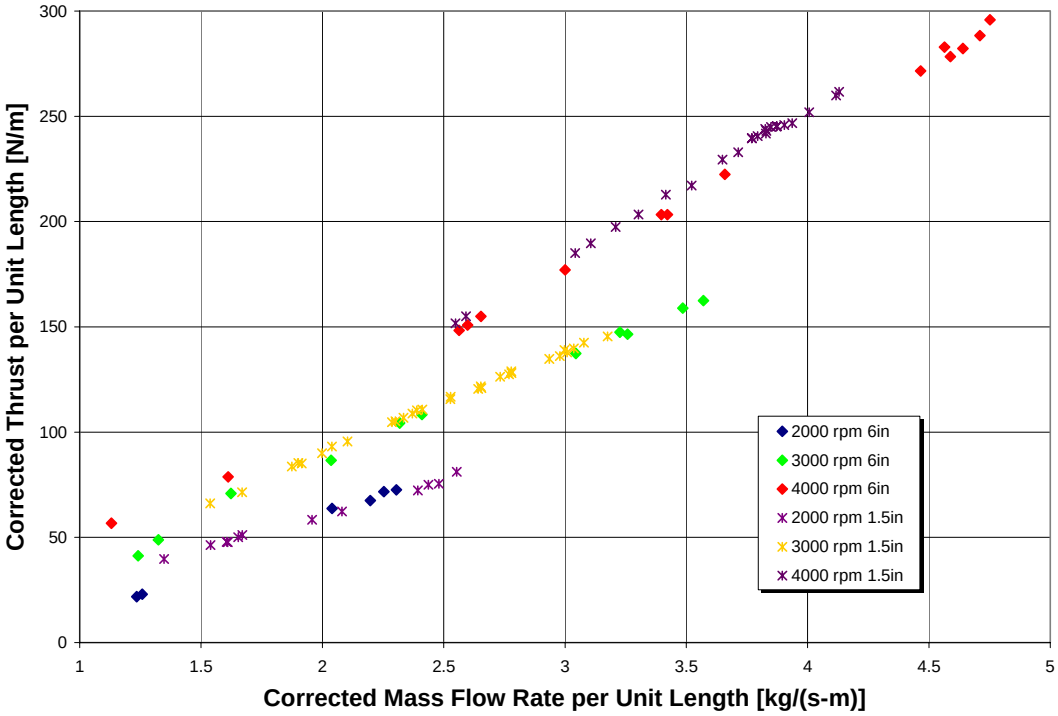

Figure 23. Comparison of corrected thrust versus corrected mass flow rate

Lastly, the thrust-to-power ratio versus mass flow rate per unit span was charted in Figure 24. Only trendlines were shown for the 6-inch fan. For the comparison at 4,500 RPM, an average of data for 4,000 and 5,000 RPM trials were made for the 1.5-inch fan in order to more accurately compare available data with the 6-inch fan. Although some scattered data for the 1.5-inch fan was present, at 3,000 RPM, the 6-inch fan appeared to hold a nearly 3 N/kW per unit length mass flow rate advantage over the shorter rotor. This average declined as operating speed was increased, showing moderate advantage at the 4,000 RPM range and only slight, if any, advantage at 4,500 RPM.

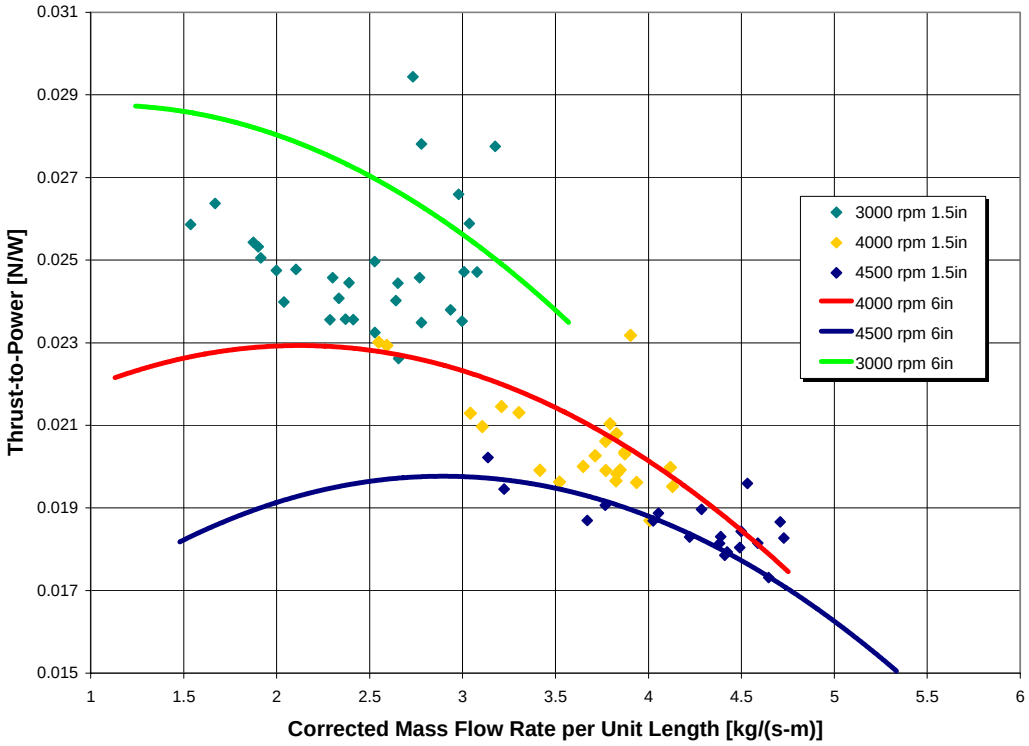

Figure 24. Comparison of thrust-to-power ratio versus corrected mass flow rate

IV. CONCLUSIONS AND RECOMMENDATIONS

A. DATA RELIABILITY

Although the experiment was prematurely ended by the failure of the test rotor during operation, a fair amount of reliable data were collected prior to that point which allowed for a reasonable performance map of the 6-inch span rotor to be generated. These data were used to determine parameters such as pressure and temperature ratios, efficiency, power into the crossflow fan, and thrust generated. Shown in the previous section, the trendlines of these parameters were similar in range and form to those determined in earlier studies by VSD [Ref. 4], Seaton and Cheng [Refs. 6, 7], and Hobson and Gannon [Ref. 9]. Furthermore, aside from scattered data found at the 2000 RPM operating speed, which was impacted by measurement inaccuracies, all other data fit the expected trends within reasonable variances. The outcome of this experiment indicated consistent performance of this crossflow fan with its earlier counterparts.

B. PERFORMANCE COMPARISON

The performance of the rotor under study outperformed a fan of similar diameter, but a quarter of its span, moderately well in efficiency, mass flow rate per unit length, and thrust-to-power ratio per unit-span mass flow rate. However, in specific thrust based on a unit-span length, no difference of performance was determined. The scaling relationships determined by comparison of performance parameters within the range of 3000 - 4500 RPM were:

- 3-9 % higher efficiencies for the 6-inch span rotor,

- 0.86 ratio of mass flow rate per unit span capacities between the shorter and longer span rotors,

- 1:1 ratio of specific thrust per unit length,

- 0.96 ratio of thrust-to-power per mass flow rate per unit-span for the 1.5-inch versus 6-inch rotor

Finally, on the structural strength of the rotor, and thus its ability to attain high speeds and maximum thrust, the shorter span rotor was superior- capable of being driven

to over 8000 RPM, while the fan under investigation failed at under 5000 RPM. Though construction methods were not meant to be fail proof or production quality at this point in the testing, such potential vulnerabilities of dimensional scaling and material composition factors must be considered when designing a crossflow fan to operate under a wide range of conditions and speeds.

C. RECOMMENDATIONS

Further studies should be made of this length of rotor to provide a complete comparison with the data available for other dimensions but similar configuration of crossflow fan. This would allow for verification of scaling relationships across a range of speeds. Also further lengthwise scaling would provide another reference point to build a more complete scaling chart. Furthermore, major configuration changes such as blade forms and housing geometries should be altered to compare their effects as well and truly determine an optimal configuration to be used in a specific aircraft arrangement.

Lastly, once enough data have been obtained to form full sets of performance characteristics and scaling charts for this and other configurations of rotors, design of a prototype craft around a selected fan should be continued. From this, the physical implications and challenges of mounting and operating such a device in a moving vehicle could be determined.

D. OUTLOOK

Though crossflow fan technology is neither new nor well developed, its characteristics have made it attractive for a number of various applications. Now in the realm of aeronautic lift, the crossflow fan has again emerged as a possible solution to geometry and weight constraints that more conventional propulsion devices may not meet. This experiment has added another series of performance data to the bank of knowledge built over the last 30 years on the crossflow fan by military research initiatives. With the impending advancements in air traffic and avionic systems enabling the reality of personal air vehicles to take form, the crossflow fan may very well have a

place in that application as well. With further study and design, a prototype aircraft using these fans for lift could well be the next breakthrough in air travel.

THIS PAGE INTENTIONALLY LEFT BLANK

APPENDIX SIX-INCH SPAN ROTOR DATA LISTING

Run #	RPM	Patm [1]	Pcal [2]	Po nozzle [3]	Pout TTR [4]	Pin TTR (8 o/c) [5]	Pin CFF (2 o/c) [6]	Pin CFF (10 o/c) [7]
1	1037.409	101289.2	118170.8	102576.554	101513.538	102588.723	101233.2518	101234.224
2	1014.566	101289.2	118170.8	102498.338	101463.735	102482.423	101221.7204	101222.8931
3	2006.563	101289.2	118170.8	103391.827	101526.719	103400.9882	100968.3281	100973.0261
4	3004.117	101289.2	118170.8	104748.161	101645.768	104775.3979	100606.6568	100613.4244
1	1998.993	101289.2	118170.8	103434.67	101562.963	103425.25	101003.4388	101004.0758
3	2999.115	101289.2	118170.8	104727.699	101631.71	104757.8196	100614.3495	100618.8107
4	3505.618	101289.2	118170.8	105600.657	101719.643	105651.3174	100350.0822	100351.6927
5	4019.782	101289.2	118170.8	106586.495	101731.057	106588.3748	100057.3371	100061.6664
1	1974.857	101289.2	118170.8	103638.509	101615.269	103651.7879	100955.9032	100956.8156
2	2048.851	101289.2	118170.8	103620.024	101564.79	103625.7517	100961.1801	100921.8637
3	3004.077	101289.2	118170.8	105124.665	101657.288	105111.9712	100376.4354	100387.2963
5	1865.044	101289.2	118170.8	104927.275	101626.032	104975.312	100398.8006	100402.0618
6	2021.982	101289.2	118170.8	104127.933	101605.38	104103.2054	101031.7416	101034.807
7	2071.604	101289.2	118170.8	104131.437	101645.102	104129.2917	101030.1663	101033.4689
8	2074.765	101289.2	118170.8	104155.89	101644.415	104153.5136	101068.9115	101073.3919
9	2082.22	101289.2	118170.8	104187.662	101653.686	104175.1677	101064.2971	101068.7449
10	2997.71	101289.2	118170.8	106621.7	101921.837	106663.3736	100805.6393	100823.9464
11	2999.835	101289.2	118170.8	106570.977	101904.155	106603.1167	100811.5078	100828.2576
12	3003.35	101289.2	118170.8	106387.004	101846.266	106379.3006	100805.7916	100814.9601
13	3010.946	101289.2	118170.8	105532.803	101769.982	105556.7921	101002.7856	101003.771
14	3013.189	101289.2	118170.8	104944.069	101662.666	104970.3789	101096.2996	101090.487
15	2990.387	101289.2	118170.8	104351.407	101568.214	104351.9163	101219.4907	101201.6127
16	3999.582	101289.2	118170.8	110248.576	102325.594	110263.4749	100410.3625	100435.5588
17	4006.119	101289.2	118170.8	109831.332	102281.662	109818.3217	100496.0569	100525.7569
18	4016.576	101289.2	118170.8	108242.224	102013.343	108275.7098	100760.6579	100773.3638
20	4009.597	101289.2	118170.8	107132.838	101870.154	107150.6249	100927.0001	100928.5675
21	4470.565	101289.2	118170.8	112499.981	102584.534	112576.2029	100215.5159	100275.894
1	2998.666	101289.2	118170.8	106499.028	101908.817	106516.2974	100843.7866	100845.4361
2	3003.48	101289.2	118170.8	106299.956	101849.329	106308.2673	100865.0937	100869.0981
3	3002.597	101289.2	118170.8	105452.71	101770.315	105473.254	101018.1144	101013.8371
4	2994.988	101289.2	118170.8	104888.627	101666.313	104880.2607	101082.1614	101071.9409
5	3005.705	101289.2	118170.8	104250.821	101567.777	104242.2872	101207.9463	101194.2857
6	4011.821	101289.2	118170.8	110157.398	102351.651	110171.5344	100464.6478	100488.8052
7	4008.58	101289.2	118170.8	109765.769	102286.57	109755.3529	100520.4371	100547.1671
8	4003.284	101289.2	118170.8	108124.917	102011.13	108119.4265	100785.516	100808.253
9	4007.723	101289.2	118170.8	106773.575	101815.379	106783.1073	100979.6259	100988.1823
10	4017.802	101289.2	118170.8	105814.807	101735.132	105823.1975	101179.033	101164.108
11	4494.417	101289.2	118170.8	112170.372	102558.144	112236.5865	100242.5211	100320.4274
12	4495.499	101289.2	118170.8	111860.981	102518.792	111847.5022	100303.7437	100376.2587
13	4503.795	101289.2	118170.8	109828.84	102175.559	109889.4646	100628.1149	100684.3904
14	4503.93	101289.2	118170.8	108373.558	101964.013	108385.826	100851.7957	100899.8497
15	4506.91	101289.2	118170.8	106731.589	101792.923	106731.9269	101142.6284	101159.9853
1	3990.08	101289.2	118170.8	110235.291	102342.728	110305.9168	100473.0724	100532.346
2	4004.522	101289.2	118170.8	109915.765	102259.737	109902.4606	100481.2528	100542.6229
3	4010.026	101289.2	118170.8	108235.568	102040.251	108273.7717	100806.7587	100830.5818
4	4010.536	101289.2	118170.8	107083.04	101876.203	107113.0013	100960.3316	100987.8746
5	4026.558	101289.2	118170.8	107092.855	101870.282	107115.5612	100954.8091	100981.883
6	4009.073	101289.2	118170.8	105757.975	101725.762	105778.2	101183.3119	101185.8315
7	4493.281	101289.2	118170.8	111601.834	102484.686	111651.826	100335.3307	100394.4389
8	4500.91	101289.2	118170.8	109651.56	102163.696	109610.4208	100671.2852	100712.827
9	4494.431	101289.2	118170.8	108144.939	101934.963	108162.5148	100870.7137	100907.1754
10	4514.66	101289.2	118170.8	106514.318	101752.5	106509.2738	101129.3672	101136.6293

Table 3. Test data listing for 6-inch span rotor

Pout CFF (Top) [8]	Pout CFF (Mid) [9]	Pout CFF (Bot) [10]	PA [11] Cell Pressure	PB [12] Outlet static	PC [13]	PD [14]	PE [15]
101335.0613	101338.95	101342.6711	101292.4535	101304.1531	101292.45	101292.7	101292.5
101337.2161	101341.1029	101349.8815	101293.6246	101306.5915	101292.89	101293	101292.7
101472.4911	101460.5111	101489.6388	101309.873	101322.5576	101297.52	101295.4	101289.5
101763.9312	101746.51	101806.3118	101290.2739	101415.9415	101290.27	101289.4	101289.8
101482.5042	101478.5818	101480.1239	101300.0302	101348.8755	101285.18	101285.2	101285.2
101778.1923	101748.037	101790.8379	101291.4156	101371.1474	101286.82	101286.8	101286.8
101980.1552	101917.9878	101986.3283	101286.8869	101457.3187	101285.75	101285.7	101285.7
102211.4391	102175.0597	102230.4007	101287.6916	101426.195	101284.47	101284.5	101284.5
101498.628	101496.2628	101489.7752	101309.2386	101276.1926	101287.17	101287.2	101287.2
101466.7017	101458.6351	101465.8883	101266.2894	101227.6508	101243.07	101243.1	101243.1
101715.8353	101682.4718	101685.8659	101252.5455	101167.4223	101228.04	101228	101228
101726.6563	101706.7486	101713.713	101255.0597	101208.8241	101232.91	101232.9	101232.9
101918.5622	101820.6057	101717.8465	101230.9927	101099.4189	101207.18	101207.2	101207.2
101951.0549	101801.9599	101744.8959	101240.5131	101104.6967	101218.35	101218.3	101218.3
102004.7873	101763.9618	101725.6403	101294.225	101220.9081	101264.8	101264.8	101264.8
102014.8438	101799.1406	101728.8581	101286.3833	101172.9465	101265.77	101265.8	101265.8
102897.0106	102284.7546	102221.3074	101293.8886	100970.8798	101262.13	101262.1	101262.1
102874.6953	102327.7261	102201.9153	101284.139	100972.0414	101266.13	101266.1	101266.1
102813.5624	102272.8239	102203.6339	101241.9271	101127.1331	101225.02	101225	101225
102651.6554	102393.171	102375.8074	101287.7742	101625.6693	101271.16	101271.2	101271.2
102472.1395	102419.3168	102381.7562	101289.5752	101866.343	101268.4	101268.4	101268.4
101977.0292	102116.2806	102169.1669	101284.8508	101797.6032	101270.54	101270.5	101270.5
104234.893	103089.0887	102984.8594	101240.1723	100686.2611	101226.26	101226.3	101226.3
104195.7736	103212.7475	103007.641	101284.0923	100946.4602	101270.2	101270.2	101270.2
103837.8664	103255.0583	103211.9669	101282.184	101852.2178	101269.72	101269.7	101269.7
103540.2323	103211.0824	103241.4077	101281.1599	102310.4178	101269.95	101269.9	101269.9
105052.672	103614.8778	103351.593	101278.8089	100590.8678	101268.52	101268.5	101268.5
102848.0533	102259.1037	102209.5532	101290.1105	100982.2046	101320.07	101320.1	101320.1
102824.1409	102283.6666	102238.6074	101286.6105	101130.8384	101320.13	101320.1	101320.1
102608.4659	102433.635	102420.3316	101288.7301	101627.6145	101319.34	101319.3	101319.3
102427.4171	102317.8928	102340.56	101287.8861	101834.4953	101292.1	101292.1	101292.1
101874.1454	101932.8353	101971.4561	101270.1105	101756.7991	101296.25	101296.3	101296.3
104221.818	103068.5427	102976.0971	101292.2381	100734.2583	101308.47	101308.5	101308.5
104139.229	103146.8498	103049.0983	101329.8864	100972.8577	101319.13	101319.1	101319.1
103787.15	103162.4018	103201.0381	101292.8059	101878.9178	101321.1	101321.1	101321.1
103460.3744	103190.5484	103211.8381	101292.3345	102403.3708	101322.42	101322.4	101322.4
102573.5927	102812.0219	102939.2716	101291.2231	102213.9106	101322.79	101322.8	101322.8
104982.9442	103582.7535	103314.5969	101290.1114	100616.6533	101323.1	101323.1	101323.1
104931.1001	103596.4772	103393.0844	101291.0213	100862.9393	101323.71	101323.7	101323.7
104531.25	103740.7965	103712.1533	101289.2016	101986.8845	101324.08	101324.1	101324.1
104142.0785	103634.782	103726.6777	101292.3693	102585.5135	101325.06	101325.1	101325.1
102919.4709	103136.2809	103350.2933	101289.9094	102459.9004	101325.8	101325.8	101325.8
104138.6692	103088.0312	102940.5354	101292.56	100755.2352	101287.09	101287.1	101287.1
104084.8387	103051.0131	102922.5807	101250.0623	100927.617	101243.83	101243.8	101243.8
103742.8801	103130.8383	103169.3785	101295.8883	101857.1929	101284.6	101284.6	101284.6
103458.4143	103146.2043	103184.1935	101293.837	102334.0889	101289.1	101289.1	101289.1
103507.5805	103173.7589	103218.0983	101293.2326	102343.7059	101289.2	101289.2	101289.2
102532.4669	102696.2403	102845.5341	101292.8971	102208.9521	101291.08	101291.1	101291.1
104853.3836	103522.0551	103392.2998	101277.5281	100886.2775	101275.44	101275.4	101275.4
104440.6936	103678.6246	103669.4154	101308.3257	102028.1137	101289.57	101289.6	101289.6
104102.7468	103617.4176	103677.9409	101292.3606	102584.0515	101292.06	101292.1	101292.1
102776.0932	102811.4288	103017.6605	101284.562	102425.4592	101285.94	101285.9	101285.9

Pout CFF [16]	PG [17]	Pin CFF (12 o/c) [18]	PI [19]	PJ [20]	PK [21]	PL [22]	Pnoz1 [24]	Pnoz2 [25]
101328.8931	101292.4	101245.1525	101312.5	101291.5	101291.4	101291.8	101218.2	101194.6
101276.771	101292.5	101240.8189	101261.2	101272.9	101283	101280.9	101259.6	101239.5
101365.3766	101294.7	101058.2613	101328.7	101262.7	101265.9	101267.5	100932.1	100836.8
101329.4382	101289.6	100854.7089	101313.2	101289.5	101289.5	101289.4	100482.3	100287.6
101373.5495	101285.2	101165.7645	101285.2	101285.2	101285.2	101285.2	100960.9	100869.2
101344.7491	101286.8	100855.5239	101286.8	101286.8	101286.8	101286.8	100485.7	100357
101333.5543	101285.7	100692.9589	101285.7	101285.7	101285.7	101285.7	100157.7	99901.83
101329.7091	101284.5	100501.3735	101284.5	101284.5	101284.5	101284.5	99769.93	99453.89
101425.6092	101287.2	101061.5964	101287.2	101287.2	101287.2	101287.2	100915.8	100772.1
101289.4387	101243.1	100997.8529	101243.1	101243.1	101243.1	101243.1	100822.3	100669.9
101264.6284	101228	100692.3888	101228	101228	101228	101228	100234.8	100008.6
101279.3156	101232.9	100710.5937	101232.9	101232.9	101232.9	101232.9	100276.1	99978.57
101229.5962	101207.2	101193.118	101207.2	101207.2	101207.2	101207.2	101126	101079.7
101238.9809	101218.3	101204.6608	101218.3	101218.3	101218.3	101218.3	101141	101087
101277.7965	101264.8	101258.5169	101264.8	101264.8	101264.8	101264.8	101215.5	101192.3
101272.2928	101265.8	101247.2355	101265.8	101265.8	101265.8	101265.8	101175.7	101178.5
101281.6611	101262.1	101267.4637	101262.1	101262.1	101262.1	101262.1	101037	100941.4
101283.9352	101266.1	101214.8293	101266.1	101266.1	101266.1	101266.1	101049.8	100939.1
101229.9296	101225	101186.4729	101225	101225	101225	101225	101091.9	100921.5
101287.2305	101271.2	101240.1685	101271.2	101271.2	101271.2	101271.2	101156.7	101140.1
101289.9152	101268.4	101242.0891	101268.4	101268.4	101268.4	101268.4	101244	101217.8
101284.307	101270.5	101269.1481	101270.5	101270.5	101270.5	101270.5	101252.6	101237.3
101239.5245	101226.3	101129.5333	101226.3	101226.3	101226.3	101226.3	100801.7	100609.9
101282.6618	101270.2	101176.4983	101270.2	101270.2	101270.2	101270.2	100879.1	100704.1
101280.9917	101269.7	101203.6996	101269.7	101269.7	101269.7	101269.7	101021.4	100903.8
101280.717	101269.9	101222.8602	101269.9	101269.9	101269.9	101269.9	101108.8	101026.9
101277.2756	101268.5	101136.9615	101268.5	101268.5	101268.5	101268.5	100729.3	100496.2
101290.1779	101320.1	101224.436	101320.1	101320.1	101320.1	101320.1	101147.6	100954.2
101289.2017	101320.1	101228.1245	101320.1	101320.1	101320.1	101320.1	101114.2	101047.3
101289.5048	101319.3	101245.6876	101319.3	101319.3	101319.3	101319.3	101167.5	101153.5
101262.5205	101292.1	101232.4662	101292.1	101292.1	101292.1	101292.1	101193.1	101184.2
101269.7057	101296.3	101252.6384	101296.3	101296.3	101296.3	101296.3	101243.2	101225.7
101278.5737	101308.5	101154.9531	101308.5	101308.5	101308.5	101308.5	100862.1	100657.3
101290.4151	101319.1	101180.8998	101319.1	101319.1	101319.1	101319.1	100904.3	100724.8
101290.2459	101321.1	101212.266	101321.1	101321.1	101321.1	101321.1	101138	100921.9
101303.8214	101322.4	101285.4962	101322.4	101322.4	101322.4	101322.4	101212.3	101073.3
101290.8188	101322.8	101260.8004	101322.8	101322.8	101322.8	101322.8	101293	101267.3
101288.4603	101323.1	101152.2591	101323.1	101323.1	101323.1	101323.1	100806.7	100555.3
101287.9886	101323.7	101154.8869	101323.7	101323.7	101323.7	101323.7	100787.3	100593.3
101288.2581	101324.1	101196.7007	101324.1	101324.1	101324.1	101324.1	100971.8	100824.5
101244.3153	101325.1	101223.0853	101325.1	101325.1	101325.1	101325.1	101083.9	101043.2
101246.1969	101325.8	101256.1729	101325.8	101325.8	101325.8	101325.8	101219.9	101248.5
101292.2578	101287.1	101175.0202	101287.1	101287.1	101287.1	101287.1	100884.7	100710.8
101248.816	101243.8	101137.4944	101243.8	101243.8	101243.8	101243.8	100868	100686.4
101281.2383	101284.6	101247.8389	101284.6	101284.6	101284.6	101284.6	101131.5	100925.4
101294.0386	101289.1	101240.9679	101289.1	101289.1	101289.1	101289.1	101170.4	101117.9
101292.6616	101289.2	101240.6972	101289.2	101289.2	101289.2	101289.2	101163.3	101114.2
101292.4604	101291.1	101267.4661	101291.1	101291.1	101291.1	101291.1	101241.8	101216.6
101275.9133	101275.4	101175.2916	101275.4	101275.4	101275.4	101275.4	100795.1	100580
101298.6125	101289.6	101245.4081	101289.6	101289.6	101289.6	101289.6	100985.7	100834.5
101291.6549	101292.1	101226.3932	101292.1	101292.1	101292.1	101292.1	101109.1	101053.3
101283.7551	101285.9	101257.6652	101285.9	101285.9	101285.9	101285.9	101216.6	101176.7

Pnoz3 [26]	Pin [31]	Pin (Flange) [32]	Pout (Flange) [33]	Pout (Vena) [34]	Tin CFF (2 o/c)	Tin CFF (12 o/c)	Tin CFF (10 o/c)
101192.7	113364.7	113381.7393	113244.6284	113277.9171	292.7066406	292.5403809	292.6155762
101229.7	113437	113472.4761	113282.3941	113220.1068	292.4439453	292.1128906	292.4517578
100820.7	113593.8	113693.9795	113510.7908	113457.3343	292.6724609	292.3973145	292.6561035
100254.6	113535.4	113557.2223	113296.2711	113438.389	293.0069336	292.6858887	293.014502
100858.5	112989.7	113021.7109	112938.8375	113036.3604	291.8016113	291.2354492	291.9742188
100325	113014.6	113066.0954	112986.6992	113022.5559	292.710791	292.4656738	292.4969238
99869.35	113169.7	113084.7611	112937.0081	112967.2364	292.7566895	292.498877	292.6797852
99425.03	113065.5	113153.6099	112926.2047	112975.5053	292.479834	292.1629395	292.509375
100766.7	113039.8	113189.0726	113090.5423	113090.9482	290.7376465	290.5291504	290.6990723
100661.2	113171.6	113144.1663	113058.1438	113065.7022	290.775	290.5787109	290.5992188
99916.2	114120	114088.2915	113992.5772	114046.8154	291.0298828	290.8416504	290.7842773
99959.58	113750	113655.7842	113949.6755	114155.679	290.3370117	290.0745605	290.3641113
101092.5	113395.9	113421.037	113247.5696	113442.9377	290.0008301	289.8628906	290.1580566
101098.5	113481.3	113392.0746	113363.1351	113393.2661	291.0420898	290.9009766	290.7491211
101144.9	113413.3	113484.4722	113356.7108	113389.568	291.0953125	290.9090332	290.7996582
101177.7	113522.9	113532.8027	113371.017	113480.2777	290.747168	290.644873	290.7242188
100980	114590.7	114658.8434	114463.6113	114612.8538	290.2762207	290.2312988	290.490332
100985.1	114646.6	114630.8812	114479.7927	114458.5928	291.1868652	291.123877	291.1426758
100959	114524.4	114723.8858	114371.7676	114513.1812	291.3077148	291.316748	291.245459
101142	114446.4	114539.455	114308.6635	114501.9752	290.3560547	290.2325195	290.6507324
101214.2	114336.4	114218.3785	114104.2353	114182.4849	290.8208984	290.6687988	290.8904785
101238.1	113842.4	113834.3008	113669.966	113717.04	290.8223633	290.3428711	291.026709
100680.5	120343.3	120358.4621	120253.6182	120150.7193	290.7269043	291.0533203	291.0640625
100764.9	119514.5	119524.0966	119405.6381	119299.0984	291.6724609	291.8121094	291.6526855
100944.8	116862	116904.395	116774.8141	116616.4498	290.6866211	290.7354492	291.130957
101053.2	116389.9	116441.6134	116353.7724	116296.6649	291.1128906	291.0220703	291.3140625
100590.1	119972	119996.1864	119707.4155	119640.8016	291.0608887	291.4200195	291.4368652
101001.5	115881.8	115967.6999	115741.3905	115933.7017	290.3284668	290.2149414	290.3431152
101025.3	116076.1	116091.6916	115834.6289	115841.0221	289.7774414	289.7881836	290.1746582
101154.9	116475.3	116496.4934	116259.6911	116427.416	290.0291504	289.8389648	290.176123
101186.9	116303.2	116397.676	116234.2161	116256.2753	290.0103516	290.0113281	290.2757324
101229.1	115130.6	115167.8712	115090.6289	115127.6656	289.8501953	289.1705078	290.1419434
100742.2	119819.2	119901.0923	119733.779	119775.9543	289.1583008	289.2928223	289.5816406
100799.8	120055.8	120086.1949	119838.1436	119836.4256	290.1819824	290.2095703	290.2271484
100979.3	118822.8	118857.4674	118650.2396	118650.9144	288.9539551	288.9568848	289.3191895
101100.4	118470.6	118579.5557	118409.8111	118406.41	290.2164063	290.1885742	290.2745117
101219.7	118388.6	118457.4161	118210.834	118378.8154	290.4314941	289.7293457	290.3624023
100645.2	120654.6	120731.2034	120486.2636	120462.8102	290.6126465	290.6355957	290.6932129
100676.8	120705.5	120684.1064	120422.9236	120387.2034	290.2474121	290.4620117	290.5008301
100882.2	120203.9	120273.6627	120014.1882	120056.7823	289.6368164	289.7562012	290.0577148
101019.7	120557.4	120699.9455	120509.1096	120449.9361	290.4895996	290.4461426	290.6695313
101242.6	119303.8	119431.1547	119194.461	119126.2477	291.0801758	290.6807617	290.9244141
100770.3	120117.4	120095.5391	119945.6599	119950.1933	290.3321289	290.1207031	290.2088379
100754.3	119396.9	119457.2559	119178.3277	119199.3122	290.6358398	290.396582	290.3812012
100979.1	116591.1	116652.4462	116371.0046	116452.4198	290.3863281	290.1355957	290.2730469
101116.9	115676.7	115874.3595	115597.0496	115606.589	291.707373	291.3465332	291.3470215
101087.1	115771.6	115723.2075	115553.846	115582.1962	291.2901367	290.9270996	291.1558594
101232	116396.7	116359.9635	116330.2989	116248.364	292.191748	291.6224121	291.7183594
100680.5	119596.5	119620.4859	119399.2933	119398.116	291.9732422	291.7684082	291.7254395
100899.9	117897.8	118009.4487	117617.4895	117721.8489	292.3013672	292.0279297	292.0486816
101056	116973.6	116970.323	116775.5464	116796.5143	291.9810547	291.7007813	291.920752
101186.5	115984.6	116003.494	115900.8822	115767.2376	292.0706543	291.3746094	291.8619141

Tin TTR (8 o/c)	Tin TTR (5 o/c)	Tout TTR	Tin Orifice	Tout CFF (Bot)	Tout CFF (Mid)	Tout CFF (Top)	TTR Mass Flow (	Turbine Power
300.3204102	299.7625488	298.5848	312.7066	292.9256348	292.8672852	292.9419922	4414.164203	157240.943
302.530127	302.3318848	301.0409	310.1837	292.5887207	292.5674805	292.663916	7003.841424	251761.438
303.1568359	303.4876465	301.3253	309.2779	293.2115234	293.1880859	293.3172363	5569.215094	200153.414
303.6697754	304.2588867	301.275	308.9105	294.1397461	294.15	294.3152832	4698.675692	168520.95
294.9495605	295.3106445	293.7462	299.4854	292.012793	292.0020508	292.057959	3302.089392	115920.306
296.6612305	296.9324707	294.6397	301.2086	293.7295898	293.6822266	293.7015137	1356.110325	47618.7175
297.3074707	297.6272949	294.7821	301.4339	294.2894043	294.2479004	294.3543457	6855.945687	240443.519
297.6355957	297.9991211	294.6427	301.5689	294.5704102	294.5379395	294.7168945	4568.843252	159900.242
293.5760254	293.7544922	292.2137	299.8463	291.302832	291.2203125	291.3018555	3456.087646	120624.958
294.3838867	294.511084	292.9757	300.4547	291.3470215	291.2737793	291.3265137	4968.330257	173832.424
295.3414063	295.5564941	293.1725	300.8656	292.3174805	292.2620605	292.3765625	4145.471154	144761.602
296.4349121	296.5298828	294.3341	300.4974	291.1578125	291.1163086	291.2103027	9764.131022	342408.451
296.0594238	296.474707	294.4313	300.8612	290.6929688	290.6941895	291.1597656	3313.596243	116427.741
296.7615723	297.1851563	295.1141	301.1568	291.8206543	291.7474121	292.045752	4531.102499	159567.297
297.0533203	297.4700684	295.3861	301.3377	291.8038086	291.7764648	292.0396484	2352.837662	82928.732
297.3050293	297.8333496	295.6688	301.2235	291.5262207	291.5079102	291.8501953	3151.516939	111197.834
297.6937012	298.3023438	294.8683	301.4059	291.7164063	291.8260254	292.5325684	2285.051613	80079.9506
298.0994629	298.6922363	295.3304	301.2503	292.757666	292.7979492	293.4200195	6652.075893	233536.858
298.248877	298.8240723	295.546	301.3148	292.8387207	292.9058594	293.4930176	1626.823762	57168.4966
298.2410645	298.8619141	295.9271	301.3529	291.8916992	291.9249023	292.3428711	3615.036752	127370.673
298.231543	298.9227051	296.182	301.4461	292.2867188	292.2217773	292.4488281	6009.772864	212120.286
298.1275391	298.86875	296.3556	301.38	291.9368652	292.0276855	292.2312988	5412.313742	191325.46
298.4744629	299.2771973	294.0917	301.5069	293.8257813	294.0293945	295.1419434	6893.883188	239666.266
298.582373	299.2486328	294.3358	301.5426	294.6277832	294.7691406	295.8040527	7265.49181	252916.893
298.6526855	299.3042969	295.0506	301.6546	293.3311523	293.5252441	294.2754883	7668.424351	268194.17
298.6282715	299.349707	295.5423	301.5516	293.6873535	293.7354492	294.1202148	4719.517624	165630.374
298.7779297	299.5359863	293.4803	301.5477	294.757666	295.1189941	296.4009766	9022.800665	312025.823
296.4285645	296.9412598	293.5453	300.6659	291.8467773	291.9219727	292.6124023	3518.871853	122736.264
296.7945313	297.3645996	294.0216	300.5614	291.3226074	291.4310059	292.1177734	7492.478771	261860.904
296.9249023	297.4651855	294.5458	300.7367	291.4588379	291.4600586	291.785498	3387.163283	118753.918
296.927832	297.5037598	294.8167	300.753	291.4375977	291.4375977	291.5860352	3350.039063	117669.049
296.8279785	297.4427246	295.0104	300.5631	290.7830566	290.8116211	290.9239258	838.9279917	29516.11
297.2388672	298.0804199	292.7381	301.0257	292.0977539	292.3157715	293.4539551	3265.747712	112957.276
297.3545898	298.1158203	293.0226	300.8067	292.9952148	293.1429199	294.1783203	7358.207583	254909.379
297.3477539	298.085791	293.7538	300.7674	291.6421875	291.7613281	292.43125	6480.189363	225634.827
297.3697266	298.1194824	294.3453	300.9417	292.5318359	292.5506348	292.7884277	3956.158545	138301.399
297.389502	298.1800293	294.8705	300.8233	292.2344727	292.4039063	292.6980957	1542.939687	54129.6723
297.7583984	298.5027832	292.4037	300.8941	294.1055664	294.4078125	295.8226074	6896.573494	237558.482
297.8575195	298.592627	292.6896	301.0057	293.93125	294.1800293	295.4905762	8881.198493	306424.349
297.9192871	298.6580566	293.5274	301.0729	293.2144531	293.3763184	294.257666	6027.280181	209124.149
297.8699707	298.6570801	294.0956	300.9518	293.5696777	293.6141113	294.0408691	5160.235765	179775.065
297.8008789	298.6502441	294.8739	300.8626	293.7835449	293.9957031	294.3814453	6598.697063	231176.278
295.2095703	295.4507813	290.6593	300.1744	292.8245605	293.0364746	294.0352539	6433.707633	220888.987
295.7347168	296.0154785	291.3355	300.4671	293.1438965	293.3030762	294.2278809	6967.352152	239902.414
296.0206055	296.316748	292.3365	300.4994	292.7659668	292.8777832	293.3924316	5769.826271	199856.933
296.2032227	296.5586914	293.0047	300.339	293.6907715	293.7137207	293.9153809	4086.664349	142120.904
296.4080566	296.7918457	293.2335	300.5052	293.4095215	293.4510254	293.7701172	6718.239782	233842.258
296.802832	297.2076172	294.2591	300.6368	293.9324707	294.0972656	294.2359375	5960.591891	208655.595
297.2911133	297.8189453	292.1695	300.8592	295.2376465	295.459082	296.5953125	6982.771188	240526.818
297.4595703	297.9366211	293.1395	300.8326	295.3143066	295.4515137	296.0831055	6530.422236	226333.542
297.5330566	297.9756836	293.8194	300.8133	294.7681641	294.8257813	295.1492676	6526.854158	227217.398
297.6167969	298.1370605	294.7716	300.8495	294.3135742	294.4285645	294.5552734	7198.583206	252174.749

CFF Mass Flow (k	Pi CFF	Tau CFF	CFF Efficiency	CFF Corrected Mass F	Corrected Power (Watts)	Corrected Speed (RPM)
0.079102089	1.000976	1.006847	0.040730041	0.079500842	157.7914742	1029.978807
0.059199886	1.001129	1.000925	0.34834878	0.059474697	15.95354685	1007.789521
0.175329285	1.004696	1.002268	0.590539027	0.176614108	116.1336269	1992.345948
0.254713227	1.010732	1.004436	0.68862276	0.257509245	331.1195135	2981.164468
0.166988276	1.004182	1.001213	0.983447776	0.167855353	59.03085933	1987.90671
0.248588409	1.010687	1.003919	0.776054141	0.251157632	285.3593425	2977.954867
0.298957642	1.014897	1.005645	0.749900125	0.302787966	495.5203205	3480.365266
0.343696861	1.019947	1.007608	0.743821751	0.348841524	769.3218654	3992.60488
0.184391592	1.004985	1.002132	0.666806917	0.18514775	114.4344328	1967.330996
0.194781885	1.004987	1.002287	0.621758697	0.195639401	129.7181009	2041.059818
0.286962806	1.012035	1.004928	0.694778967	0.289705424	413.8462478	2991.443759
0.28541145	1.012058	1.003111	1.102725247	0.287775841	259.5032321	1859.204412
0.353472038	1.007246	1.002902	0.711405525	0.354192359	137.9650416	2016.52446
0.353050977	1.007352	1.003348	0.625765667	0.354302791	159.1887706	2062.848952
0.344900102	1.0069	1.003226	0.609551064	0.345993736	149.811707	2065.866366
0.321500743	1.007128	1.003174	0.640010877	0.322415066	137.3381827	2074.105101
0.539946695	1.014876	1.005829	0.725290133	0.541998707	424.008092	2987.941121
0.52592361	1.015023	1.006322	0.675262448	0.528739924	448.6309138	2985.854887
0.486966787	1.014804	1.006142	0.684968274	0.48976736	403.7415998	2988.643479
0.366349502	1.013764	1.005647	0.69293308	0.367367838	278.431549	3000.724657
0.246835669	1.01267	1.005247	0.686799706	0.247535445	174.3012363	3000.992497
0.200010155	1.00847	1.004591	0.525541666	0.200382867	123.4543934	2978.604787
0.715298293	1.027596	1.011632	0.671235592	0.720970152	1125.490547	3982.334705
0.686872709	1.027194	1.0115	0.669145295	0.692716276	1069.085606	3983.617224
0.55472298	1.024996	1.009832	0.719946246	0.557620461	735.7848382	3999.924344
0.454163503	1.022814	1.009267	0.697702874	0.456256751	567.4254868	3990.925018
0.795979623	1.034449	1.014143	0.687496271	0.803708217	1525.511991	4448.552015
0.492899703	1.014536	1.006309	0.654826904	0.494713557	904.8124157	2989.0896
0.462046551	1.014471	1.0059	0.697186358	0.463367016	792.4547955	2995.860711
0.351973557	1.013799	1.005356	0.732412878	0.352674136	547.5966171	2994.45671
0.308331691	1.012193	1.004784	0.724982004	0.308879495	428.3915772	2986.432779
0.18895813	1.006993	1.003861	0.516177117	0.189003242	211.5496914	2999.07464
0.715422722	1.027004	1.01133	0.67447118	0.718790036	2360.77309	4005.57005
0.702425436	1.026755	1.011139	0.679776016	0.706453291	2281.153149	3996.391953
0.516574593	1.024255	1.009922	0.692438402	0.517569784	1488.676324	3998.903251
0.394561249	1.021795	1.00826	0.748105624	0.39552275	947.0103545	3995.397687
0.172370642	1.01555	1.007827	0.564497002	0.172575626	391.5436007	4005.805843
0.766342968	1.033691	1.014215	0.66914998	0.772685839	3184.004719	4477.352547
0.756904598	1.033415	1.014223	0.663329544	0.762546865	3144.11851	4480.308974
0.613765067	1.031321	1.013109	0.675116419	0.616338359	2342.178314	4493.118709
0.480763827	1.02815	1.011036	0.721515864	0.482634767	1544.095085	4487.694968
0.224196721	1.019262	1.010858	0.503404553	0.224775421	707.4790075	4487.881479
0.691255224	1.026431	1.010606	0.705325075	0.695392921	2138.097362	3977.849609
0.67460481	1.026135	1.010628	0.696112987	0.678978254	2091.839736	3990.5269
0.519328462	1.023632	1.009464	0.707476101	0.521261101	1430.074005	3997.4302
0.38785522	1.021767	1.007913	0.779901194	0.389712734	893.9264761	3989.68576
0.403518027	1.022172	1.00831	0.756335114	0.405227892	976.1547355	4007.980743
0.243777348	1.014615	1.00769	0.540140959	0.244742019	545.6109216	3985.653359
0.746970473	1.032668	1.013507	0.683080476	0.754199562	2953.070121	4467.197907
0.615419472	1.030265	1.011948	0.716016528	0.620210649	2148.133348	4472.454703
0.455604102	1.027702	1.010439	0.750760897	0.45837984	1387.147673	4467.997911
0.294011885	1.016742	1.009128	0.520873786	0.295247542	781.2904099	4488.85957

Exit mass flow [kg/s]	Corrected exit mass flow [k	RPM	m_dot_rpm_scale	PR_rpm_scale	Power_rpm_scale	PR_m.avg	TR_m.avg	ETA_m.avg
8.684994991	8.728775978	1000	0.077186872	1.000920414	144.4104653	1.001003	1.001018	0.286393138
*err	*err	1000	0.059014998	1.001111313	15.5864689	1.001136	1.00094	0.351170638
16.0373254	16.15484786	2000	0.177292612	1.004732614	117.477237	1.004723	1.002296	0.597062766
*err	*err	3000	0.259136235	1.010868364	345.8067722	1.010783	1.004461	0.700245535
14.31642443	14.3907617	2000	0.16887649	1.004233237	61.66443323	1.004185	1.001226	0.990928859
*err	*err	3000	0.253016896	1.010845683	298.0004668	1.01073	1.003933	0.790285425
*err	*err	3500	0.304496166	1.01506509	515.8902763	1.014976	1.005676	0.763171657
*err	*err	4000	0.34948765	1.02002112	791.1685891	1.020001	1.007648	0.755056556
4.442516061	4.460734052	2000	0.188222267	1.005152016	123.3547143	1.004983	1.002163	0.668658063
6.303823971	6.331576213	2000	0.191703741	1.004787932	124.74549	1.004995	1.002312	0.627155976
4.786672816	4.832420969	3000	0.290534051	1.012104038	425.3817732	1.012058	1.004962	0.703555027
7.603532709	7.666521503	2000	0.309568801	1.013953571	329.0407932	1.012074	1.003138	1.11416432
29.82797009	29.88875481	2000	0.35128992	1.007127499	306.6825118	1.007297	1.003034	0.697465896
29.55522339	29.66001744	2000	0.343508225	1.006910794	326.1695879	1.00746	1.003443	0.628393037
28.0610611	28.15003914	2000	0.33496236	1.006467346	306.1586098	1.007144	1.003324	0.623497769
28.99430985	29.07676737	2000	0.310895591	1.006627966	279.1191151	1.007329	1.003293	0.645424547
41.73539127	41.89400234	3000	0.544186132	1.014996739	976.2860984	1.015502	1.006078	0.737647364
42.19261347	42.41855432	3000	0.531244763	1.015165534	1030.113479	1.015562	1.006541	0.687978937
42.15142618	42.39384143	3000	0.491628423	1.014916845	924.642063	1.015364	1.006354	0.69935417
42.32906888	42.44673023	3000	0.36727912	1.013757421	621.0974567	1.013994	1.005776	0.701000075
41.60708614	41.72504165	3000	0.247453579	1.012661268	385.2381083	1.012692	1.005312	0.691696359
34.36698694	34.43102863	3000	0.20182221	1.008592012	272.5167995	1.00856	1.00454	0.546619849
57.29925073	57.75359722	4000	0.724168314	1.02784161	2577.180898	1.028777	1.012021	0.689095295
57.54376761	58.03332101	4000	0.695565098	1.027417696	2448.491673	1.028192	1.011867	0.683998595
57.23474816	57.53370199	4000	0.557631008	1.024996742	1647.542687	1.02556	1.010072	0.731348934
55.90207728	56.15973098	4000	0.457294236	1.022917419	1265.317502	1.023119	1.00938	0.710861158
64.31662045	64.94110505	4500	0.813003189	1.035250338	3569.228357	1.035966	1.014603	0.70721272
41.3150331	41.46707099	3000	0.496519298	1.014641971	959.3335899	1.015133	1.006551	0.668084302
41.69402375	41.81317949	3000	0.464007236	1.014510787	835.3153659	1.015022	1.00614	0.707686853
42.40777517	42.49218492	3000	0.353327	1.01384969	564.9257843	1.013932	1.005446	0.740226651
40.06220025	40.13337759	3000	0.310282719	1.012304398	441.8784554	1.012286	1.004823	0.737467687
31.31421046	31.32168644	3000	0.189061559	1.006997672	212.7137073	1.007039	1.003848	0.530549208
56.5018477	56.76778762	4000	0.717790503	1.026928674	2451.090143	1.028207	1.011734	0.692101594
56.00679854	56.32795326	4000	0.707091096	1.02680338	2384.157848	1.027759	1.011499	0.695142791
56.40026104	56.50891724	4000	0.517711734	1.024268288	1531.981701	1.02489	1.010144	0.70727415
55.47725203	55.61244376	4000	0.395978354	1.021845408	967.7328683	1.02204	1.00833	0.763424031
46.8086954	46.86436058	4000	0.172325502	1.015504641	389.2945919	1.015736	1.007742	0.58777684
63.81370383	64.34187735	4500	0.776594257	1.034032696	3387.005584	1.035166	1.014729	0.68576453
63.93566384	64.4122656	4500	0.76589827	1.033709229	3326.84359	1.034827	1.014701	0.680520632
64.40299437	64.67301257	4500	0.617282293	1.031417352	2425.752547	1.032109	1.013403	0.688805177
62.53554411	62.77890734	4500	0.483958127	1.028304812	1593.110032	1.028667	1.011173	0.738612207
52.19375104	52.32847437	4500	0.225382377	1.019366527	715.2849696	1.019532	1.010759	0.52425944
56.28421426	56.62111885	4000	0.69926517	1.02672573	2266.972159	1.027497	1.010953	0.722956683
56.5862016	56.95304834	4000	0.680590079	1.02625948	2195.931402	1.02722	1.010961	0.715210659
55.84150046	56.04931017	4000	0.5215962	1.02366284	1472.503417	1.024252	1.009631	0.726023717
54.99183481	55.2552013	4000	0.390720229	1.021880086	920.4945181	1.022062	1.007973	0.798413345
55.5478587	55.783237	4000	0.404420997	1.022083788	994.1614887	1.022492	1.008406	0.771942937
45.43955817	45.61937066	4000	0.245622985	1.014720348	554.7317508	1.014808	1.007618	0.562286488
63.2034293	63.81510435	4500	0.759737558	1.033149659	3157.298938	1.034078	1.013915	0.703688315
63.03584607	63.52659414	4500	0.62403045	1.030639382	2262.450488	1.03103	1.012155	0.734278766
62.08973926	62.46801696	4500	0.461662991	1.028100247	1453.072874	1.02819	1.010541	0.769998947
48.31274923	48.51579527	4500	0.295980286	1.016824964	795.4850488	1.016972	1.009088	0.539794353

Thrust Calculation	To_in	Po_in	T_out	P_out	PA [11] Cell Pressure	Cp	Gamma	R gas	rho [kg/m^3]
	292.6209	101237.5	292.9186	101339	101292.4535	1005	1.41	287	1.20505328
	292.3362	101228.5	292.611	101343.4	101293.6246	1005	1.41	287	1.20634535
	292.5753	100999.9	293.2472	101476.9	101309.873	1005	1.41	287	1.20432605
	292.9024	100691.6	294.209	101777.4	101290.2739	1005	1.41	287	1.20125641
	291.6704	101057.8	292.0281	101480.7	101300.0302	1005	1.41	287	1.20928335
	292.5578	100696.2	293.7085	101776.7	101291.4156	1005	1.41	287	1.20331093
	292.6451	100464.9	294.3062	101969.5	101286.8869	1005	1.41	287	1.20148992
	292.384	100206.8	294.6203	102211	101287.6916	1005	1.41	287	1.20104147
	290.6553	100991.4	291.284	101494.7	101309.2386	1005	1.41	287	1.21249911
	290.651	100960.3	291.3229	101464.6	101266.2894	1005	1.41	287	1.21186822
	290.8853	100485.4	292.3287	101697	101252.5455	1005	1.41	287	1.20838597
	290.2586	100503.8	291.1693	101717.3	101255.0597	1005	1.41	287	1.21328944
	290.0073	101086.6	290.8872	101824.2	101230.9927	1005	1.41	287	1.21463213
	290.8974	101089.4	291.899	101843.6	101240.5131	1005	1.41	287	1.21057
	290.9347	101133.6	291.9016	101856.1	101294.225	1005	1.41	287	1.21105798
	290.7054	101126.8	291.6628	101867.9	101286.3833	1005	1.41	287	1.21202368
	290.3326	100965.7	292.0972	102530.9	101293.8886	1005	1.41	287	1.21257005
	291.1511	100951.5	293.0557	102522.5	101284.139	1005	1.41	287	1.20849294
	291.29	100935.7	293.1407	102486.5	101241.9271	1005	1.41	287	1.20766186
	290.4131	101082.2	292.0906	102496.8	101287.7742	1005	1.41	287	1.21242809
	290.7934	101143	292.338	102426.7	101289.5752	1005	1.41	287	1.21117628
	290.7306	101230.1	292.0504	102096.6	101284.8508	1005	1.41	287	1.21119134
	290.9481	100658.5	294.4456	103555.1	101240.1723	1005	1.41	287	1.20592683
	291.7124	100732.8	295.1742	103572.6	101284.0923	1005	1.41	287	1.20337963
	290.851	100912.6	293.7804	103491.9	101282.184	1005	1.41	287	1.2087986
	291.1497	101026.1	293.8807	103361.7	101281.1599	1005	1.41	287	1.20793502
	291.3059	100542.8	295.5599	104158.9	101278.8089	1005	1.41	287	1.20373884
	290.2955	100971.2	292.1973	102499.2	101290.1105	1005	1.41	287	1.21201332
	289.9134	100987.4	291.6935	102504.5	101286.6105	1005	1.41	287	1.21409554
	290.0147	101092.5	291.5942	102501	101288.7301	1005	1.41	287	1.21451474
	290.0991	101128.9	291.4984	102371.4	101287.8861	1005	1.41	287	1.21445962
	289.7209	101218.3	290.8358	101930.7	101270.1105	1005	1.41	287	1.21554967
	289.3443	100702.8	292.7395	103543.3	101292.2381	1005	1.41	287	1.21335736
	290.2062	100749.5	293.5434	103546.2	101329.8864	1005	1.41	287	1.21036331
	289.0767	100935.3	292.0091	103447.7	101292.8059	1005	1.41	287	1.21607026
	290.2265	101084.4	292.6441	103312.3	101292.3345	1005	1.41	287	1.21296577
	290.1744	101201.3	292.4208	102793.8	101291.2231	1005	1.41	287	1.21210762
	290.6472	100571.7	294.9281	104108.5	101290.1114	1005	1.41	287	1.20624304
	290.4034	100611.6	294.6727	104115.6	101291.0213	1005	1.41	287	1.20732052
	289.8169	100836.4	293.7014	104074.1	101289.2016	1005	1.41	287	1.21115729
	290.5351	100991.6	293.7812	103886.7	101292.3693	1005	1.41	287	1.21022062
	290.8951	101186.3	294.0249	103162.6	101289.9094	1005	1.41	287	1.20673988
	290.2206	100726.8	293.3995	103496.5	101292.56	1005	1.41	287	1.21047154
	290.4712	100720.5	293.6552	103462.1	101250.0623	1005	1.41	287	1.20894045
	290.265	100961.7	293.0605	103410.3	101295.8883	1005	1.41	287	1.21160617
	291.467	101063.1	293.7908	103292.8	101293.837	1005	1.41	287	1.20817731
	291.1244	101059.1	293.5715	103332.2	101293.2326	1005	1.41	287	1.20920908
	291.8442	101212.2	294.0674	102711	101292.8971	1005	1.41	287	1.20505213
	291.8224	100635	295.883	104064.5	101277.5281	1005	1.41	287	1.20209626
	292.126	100876.5	295.6769	104006.7	101308.3257	1005	1.41	287	1.20299963
	291.8675	101001.4	294.9441	103848.7	101292.3606	1005	1.41	287	1.20532066
	291.7691	101174.6	294.4207	102891.7	101284.562	1005	1.41	287	1.20415141

V [m/s]	Thrust [N]	Thrust_rpm_scale [N]	N/W	Thrust/unit length	mdot/unit length	Power/Unit length
8.872901	0.705403	0.684871472	0.0047425	4.493907	0.506476	156.6697093
9.170117	0.54539	0.541174446	0.0347208	3.551013	0.387238	108.1631862
16.80203	2.967475	2.978875508	0.025357	19.54643	1.163337	785.3077842
28.71208	7.393626	7.440340135	0.0215159	48.82113	1.700369	2226.601881
17.43813	2.927084	2.944890941	0.0477567	19.32343	1.108113	397.3267354
28.63489	7.19187	7.245110008	0.0243124	47.54009	1.660216	1912.592937
33.97369	10.28682	10.34485833	0.0200524	67.87965	1.998006	3328.455228
39.50352	13.78047	13.80599254	0.0174501	90.5905	2.293226	5162.6549
17.64332	3.266621	3.320865591	0.0269213	21.79046	1.235054	770.3943718
18.24945	3.570311	3.498487715	0.028045	22.95596	1.257899	869.9956839
27.34673	7.922496	7.945156696	0.0186777	52.13357	1.906391	2767.40469
27.83056	8.008963	8.615473588	0.0261836	56.53198	2.031291	1734.42775
31.5037	11.15837	11.06693328	0.036086	72.61767	2.305052	2062.645248
31.81787	11.27316	10.92970014	0.0335093	71.71719	2.253991	2348.393108
30.7092	10.62519	10.2864266	0.0335984	67.49624	2.197916	2214.002966
31.22629	10.06783	9.708115334	0.0347813	63.70154	2.039997	2042.710891
45.48118	24.65074	24.75022576	0.0253514	162.4031	3.570775	6329.136755
45.58342	24.10177	24.21595052	0.023508	158.8973	3.485858	6664.114189
45.71258	22.38853	22.47360471	0.0243052	147.4646	3.225908	5998.563299
44.96953	16.52036	16.51636917	0.0265922	108.3751	2.409968	4078.396641
43.63896	10.80219	10.79861769	0.028031	70.85707	1.623711	2530.318782
36.89097	7.392317	7.445416141	0.0273209	48.85444	1.324293	1750.18194
62.27353	44.89735	45.09651405	0.0174984	295.9089	4.751761	16687.57529
61.98576	42.93855	43.11513223	0.0176089	282.9077	4.564075	15869.6188
60.78045	33.89242	33.89306403	0.0205719	222.3954	3.658996	10810.03415
59.01191	26.92458	26.98580828	0.0213273	177.0722	3.000618	8246.226874
69.4563	55.8226	56.4681948	0.0158208	370.5262	5.334667	22626.00325
44.97741	22.25093	22.33215084	0.0232788	146.5364	3.258001	6226.410078
45.10183	20.8987	20.92757368	0.0250535	137.32	3.044667	5458.415503
44.99033	15.86693	15.89629928	0.0281387	104.3064	2.318419	3686.351834
42.54385	13.14092	13.20062283	0.0298739	86.61826	2.035976	2860.304881
33.22966	6.280514	6.282451796	0.0295348	41.22344	1.240561	1394.468052
61.22729	44.00956	43.94836414	0.0179301	288.3751	4.709911	16150.55072
60.83169	42.97475	43.01354397	0.0180414	282.2411	4.639705	15601.78511
59.84746	30.97523	30.98373001	0.0202246	203.3053	3.397059	10044.10693
58.03206	22.953	22.97943821	0.0237456	150.7837	2.598283	6328.06006
50.11287	8.648259	8.635724813	0.022183	56.66486	1.130745	2565.565559
68.64358	53.03992	53.30820915	0.015739	349.7914	5.095763	21890.58061
68.68857	52.37825	52.60845376	0.0158133	345.1998	5.025579	21544.36858
68.1008	41.97314	42.0374188	0.0173296	275.8361	4.050409	15844.10334
65.77563	31.74561	31.83265241	0.0199815	208.8757	3.175578	10367.95859
56.03455	12.59519	12.62920108	0.0176562	82.86877	1.478887	4655.654335
60.66011	42.18261	42.41750508	0.0187111	278.3301	4.588354	14629.3936
60.80808	41.28737	41.38537855	0.0188464	271.5576	4.465814	14306.86754
59.39611	30.96088	30.98078366	0.0210395	203.286	3.422547	9643.485631
57.84479	22.54285	22.60112973	0.0245532	148.3014	2.563781	5993.387222
58.39177	23.66197	23.61485694	0.0237535	154.9531	2.653681	6562.493304
48.83305	11.9515	11.9945195	0.0216222	78.7042	1.611699	3600.946394
68.3811	51.57299	51.95168845	0.0164545	340.8903	4.985155	20267.43433
67.27157	41.72254	41.97950771	0.0185549	275.4561	4.094688	14574.52561
65.42897	29.99132	30.20613263	0.0207878	198.203	3.029285	9332.62405
51.98903	15.34963	15.3877267	0.0193438	100.9693	1.942128	5181.047458

THIS PAGE INTENTIONALLY LEFT BLANK

LIST OF REFERENCES

1. NASA Ames, "Virtual Pathways," [http://www.nasa.gov/centers/ames/news/ releases/2003/ 03_35AR.html], (May 2006).

2. Moller International, [http://www.moller.com/skycar/safety/], (June 2006).

3. Fanwing Ltd, [www.fanwing.com], (June 2006).

4. Vought Systems Division, “One and One-Half Inche Span Fan Test,” Vol. I, “Twelve Inch Span Fan Test,” Vol. II, “Multi-Bypass Ratio Propulsion System Technology Development,” Vol. IV, prepared under contract N00019-74-C-034 for Naval Air Systems Command, July 1975.

5. Gossett, D.H., “Investigation of Cross Flow Fan Propulsion for Lightweight VTOL Aircraft,” Master’s Thesis, Department of Aeronautics and Astronautics, Naval Postgraduate School, Monterey, CA, December 2000.

6. Seaton, M. S., “Performance Measurements, Flow Visualization, and Numerical Simulation of a Cross-Flow Fan,” Master’s Thesis, Department of Aeronautics and Astronautics, Naval Postgraduate School, Monterey, CA, March 2003.

7. Cheng, W-T., “Experimental and Numerical Simulation of a Cross-Flow Fan,” Master’s Thesis, Department of Mechanical and Astronautical Engineering, Naval Postgraduate School, Monterey, CA, December 2003.

8. Hobson G. V., Cheng W. T., Seaton M. S., Gannon A. and Platzer M. F., “Experimental and Computational Investigation of Crossflow Fan Propulsion for Lightweight VTOL Aircraft,” ASME paper GT2004-53468 presented at TURBO EXPO June, 2004.

9. Gannon A., Utschig J.M., Hobson G.V., and Platzer M.F., "Experimental Investigation of a Small-Scale Cross-Flow Fan for Aircraft Propulsion," presented February 2006.

10. White, F. M., *Fluid Mechanics*, WCB/McGraw-Hill, San Francisco, 1999.

THIS PAGE INTENTIONALLY LEFT BLANK

INITIAL DISTRIBUTION LIST

1. Defense Technical Information Center
   Ft. Belvoir, Virginia

2. Dudley Knox Library
   Naval Postgraduate School
   Monterey, California

3. Dr. Garth Hobson
   Department of Mechanical and Astronautical Engineering
   Naval Postgraduate School
   Monterey, California

4. Prof. Knox Millsaps
   Department of Mechanical and Astronautical Engineering
   Naval Postgraduate School
   Monterey, California

5. Charla Schreiber
   San Diego, California